

THE PENNSYLVANIA STATE UNIVERSITY
COLLEGE OF EARTH AND MINERAL SCIENCES

DEPARTMENT OF GEOSCIENCES

Carbon, Nitrogen and Manganese in Shale Soil Profiles along a Climate Gradient

A Senior Thesis in Geosciences

by

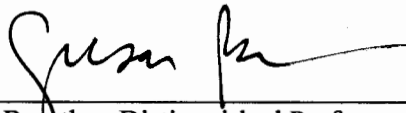
Nina Lynn Bingham

Submitted in partial fulfillment
of the requirements
for the degree of

Bachelor of Science

Spring 2013

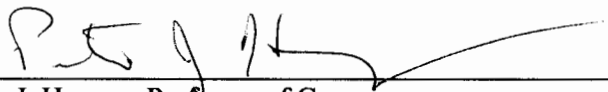
Reviewed and approved by:



Susan Brantley, Distinguished Professor of Geosciences

4-26-13

Date



Peter J. Heaney, Professor of Geosciences
Associate Head for Undergraduate Programs

April 26, 2013

Date

ABSTRACT

Addition profiles show a net enrichment of an element, j , at the surface compared to the parent material. The excess concentration of the element is coming from an outside source where it is deposited on the surface and then subsequently incorporated into the soil profile through a variety of processes. The shape of these profiles can give clues to what processes are occurring in the soil and therefore have the largest effect on the element of interest (j). Carbon and nitrogen are elements associated with organic matter. Most of their deposition to soils can be attributed to the decay of plant litter on the surface. Manganese is often used in metal refineries and input into the atmosphere via emissions; it is eventually “rained out” onto the soil during precipitation events. We analyzed the elemental concentrations of C, N and Mn in soils along a climosequence that extends through the Appalachians of the United States and includes end members in Wales and Puerto Rico. C and N display addition profiles at every sample site. Mn only displays addition profiles in Pennsylvania and Virginia. We also determined the net added or lost mass of C, N and Mn at each sample site with respect to the soil parent material. These values were compared against the mean annual temperature for each site. We saw an increase in enrichment until $\sim 11^{\circ}\text{C}$ (after the Virginia site) and then a decrease in enrichment until eventually every element studied was partially depleted at our end member in Puerto Rico. We then fit our concentration profiles with a previously described diffusion based soil mixing model to determine what soil processes were acting on C, N and Mn concentrations in the soils along our transect. We discovered that soil mixing does not trend with mean annual temperature, but higher precipitation sites had higher soil mixing rates. We also observed that the model provided a net input rate for C and N that includes an organic matter decomposition rate. We concluded that the latitude range which the soil decomposition rate overtakes the true C and N input rates occurs between VA and TN. This is the divide between increasing net mass of C, N and Mn in the soil

and decreasing net mass. The model did a good job explaining accurately the transport and storage of Mn in the soil assuming Mn is relatively immobile. Mn additions showed no trend with climate. This is expected as Mn is associated with point source pollution. A more complete (more processes incorporated) model is necessary to better quantify the soil processes associated with C and N storage and subsequently explain trends in SOM storage with temperature.

TABLE OF CONTENTS

Section Title	Page Number
List of Figures	iv
List of Tables	v
Acknowledgements	vi
Introduction	1
Methods	3
Results	10
Discussion	19
Conclusion	32
Appendix	34
Works Cited	40
CV	42

LIST OF FIGURES

Figure Number: Name	Page Number
Figure 1a: Spatial map of the sampling locations	4
Figure 1b: Latitude of sample sites vs. MAT of the sample locations	4
Figure 2: C concentration vs. profile depth for each sample site	11
Figure 3: N concentration vs. profile depth for each sample site	12
Figure 4: Mn concentration vs. profile depth for each sample site	13
Figure 5: C τ values vs. profile depth for each sample site	14
Figure 6: N values vs. profile depth for each sample site	15
Figure 7: Mn values vs. profile depth for each sample site	16
Figure 8: Mj for C, N and Mn at each sample site vs. MAT	17
Figure 9: mj for C, N and Mn at each sample site vs. MAT	18
Figure 10: C/N ratio vs. profile depth for each sample site	19
Figure 11: Model fits to C & N concentration profiles at Wales	23
Figure 12: Model fits to C, N & Mn concentration profiles at PA	24
Figure 13: Model fits to C, N & Mn concentration profiles at VA	25
Figure 14: Model fits to C & N concentration profiles at Tennessee	26
Figure 15: Model fits to C & N concentration profiles at Alabama	27
Figure 16: Model fits to C & N concentration profiles at PR	28
Figure 17: D_{eff} values from model fits for each site vs. MAT	29
Figure 18: C & N input rates from model fits for each site vs. MAT	30
Figure 19: Full C, N & Mn concentration profiles, textual and taxonomic data for Wales	34

Figure 20: Full C, N & Mn concentration profiles, textual and taxonomic data for Pennsylvania	35
Figure 21: Full C, N & Mn concentration profiles, textual and taxonomic data for Virginia	36
Figure 22: Full C, N & Mn concentration profiles, textual and taxonomic data for Tennessee	37
Figure 23: Full C, N & Mn concentration profiles, textual and taxonomic data for Alabama	38
Figure 24: Full C, N & Mn concentration profiles, textual and taxonomic data for Puerto Rico	39

LIST OF TABLES

Table Number: Name	Page Number
Table 1: Sample site descriptions	5

ACKNOWLEDGEMENTS

I would like to thank my friends and family for obligingly listening to me explain addition profiles and mathematical models even when you didn't have any idea what I was saying. I would also like to thank Megan Carter-Thomas and the rest of the Brantley Lab Group for their unending support. I would like to also thank Ashlee Dere; without her I could not have done any of this. And finally I would like to thank my adviser, Sue Brantley, who provided guidance and inspiration but also had much tolerance along the way.

1. Introduction

Soils are dynamic; a variety of physical, chemical and biological processes act upon them over varying timescales. Due to the changes occurring in soils, it is of great importance to track how these changes affect nutrients, toxins and trace metals in soils. Some elements form addition profiles in soil, meaning an element increases in concentration from the basal layer of soil to the surface (Yaalon and Ganor 1973; Brantley and Lebedeva 2011). These additions are indicators of concentrations in the soils that are in excess of what is expected based on the composition of the parent rock (protolith). This can be beneficial for ecosystems in terms of essential elements for plant growth and soil productivity: carbon (C) and nitrogen (N) for example. Conversely, excessive concentrations of certain elements in the soil can be negative in the case of toxin build ups, as is the case with manganese (Mn).

Mn is toxic to humans in varied quantities; it can cause brain degeneration when animals are exposed to high levels of manganese (U.S E.P.A. 2003). During the most recent century, Mn was used heavily in the production of steel, iron and ferromanganese alloys. The Mn was released into the air from factory emissions and accumulated in the soil during precipitation events (Herndon et al. 2011). In contrast, carbon and nitrogen owe much of their input to soils by natural cycles which include surficial input from leaf litter and fixation by plants and microorganisms at depth. Soil organic matter (SOM), which is predominantly made up of the elements C and N, has previously been shown to be highly influenced by temperature changes (Jobbagy and Jackson 2000; Davidson and Janssens 2006).

There are many concerns with how global warming will affect our environment, including concerns for how the soils we live on and rely upon for food will change. Changes in soils may impact the storage or transport of many elements and compounds held in the soil. Determination of how C, N and Mn concentrations change in a warming climate could provide important information for better management of agricultural practices, carbon sequestration studies and

prevention of toxicity events. In this thesis I target a climosequence: a set of soil sample sites along a latitudinal transect that vary with respect to mean annual temperature, MAT, and mean annual precipitation, MAP. This climosequence is used in this study as a proxy for investigating the effect of global warming on soil processes. Importantly, the climosequence used in this study is underlain by similar parent material: organic-poor Rose Hill shale. Shale, compared to other rocks, is relatively limited in its mineralogical make-up, thus providing a simple parent material (Dere et al. 2013).

Models provide another method of analyzing field data and if properly implemented can add to our understanding of the processes observed in soils. Due to the importance of SOM dynamics in agricultural practices, the leading SOM models are quite extensive. Today's models for SOM incorporate variables that include meteorological data, plant material information, soil texture, atmospheric and soil nitrogen input and soil chemistry data. The most notable of large SOM models are CENTURY and DAYCENT, which run on either month or day timescale (Parton et al. 1998; Parton et al. 1996). These models produce highly accurate descriptions for the typical grassland agricultural system and have the ability to provide model descriptions of forest landscapes; however, the complexity of the model prevents the application to smaller scale studies with limited data.

The task of creating a simpler model without forgoing accuracy has also been explored in detail over the years. Modeling relatively immobile elements such as lead and in some cases Mn has been successful using simple advection-diffusion or just diffusive-like mixing models (Kaste et al. 2007; Drivas et al. 2011). Simpler models for SOM and specifically C and N have evolved over time through the pursuit of trends of soil carbon storage with temperature, soil texture and vegetation (Jobbagy and Jackson 2000; Davidson and Janssens 2006). Presently, models by Braakhekke (2011), Baisden et al. (2002) and Elzein and Balesdent (1994) have all incorporated from three to five carbon pools as well as processes such as diffusion, advection and SOM

decomposition to move C (and N) between pools throughout the entire profile and out of the profile. Each pool of SOM contains C, N or both and has a different rate of decomposition. The models simulate the variety in SOM residence times observed in natural environments: rapid turnover on a yearly scale, medium-slow turnover on a decadal scale, and finally an almost stable pool of C with a millennial scale turnover rate (Braakhekke et al. 2011; Baisden et al. 2002; Elzein and Balesdent 1995). Generally, the rapidly decomposing pool is most often associated with surficial C pools while the stable C pool is associated with deeper depths of C stored in the mineral structure. For this study, we want to utilize the simplest model possible to fit C, N and Mn concentration profiles we observed from our data. A simple model will allow us to examine one process (soil mixing) and if this process provides an adequate explanation for the observed profiles or if there is a need for other parameters or soil processes. In this study we will apply the diffusive-mixing model as described by Drivas et al (2011) to our Mn, C and N concentration data to help explain trends seen between net C, N and Mn masses in profiles and climate variables (MAT and MAP).

2. Methods

2.1 Sample locations and collection techniques

Soil samples were taken from six sites which form a climosequence over a 34° latitudinal spread; the temperatures range between 7.2 °C – 24 °C. There are four sites on the east coast of the United States -- Pennsylvania (PA), Virginia (VA), Tennessee (TN) and Alabama (AL) -- and a cold, wet end member in Wales (W) and a warm, wet end member in Puerto Rico (PR). Figure 1a shows a map of the sample locations for reference. Figure 1b shows latitude of the sample sites plotted against mean annual temperature (MAT) to better portray the climosequence.

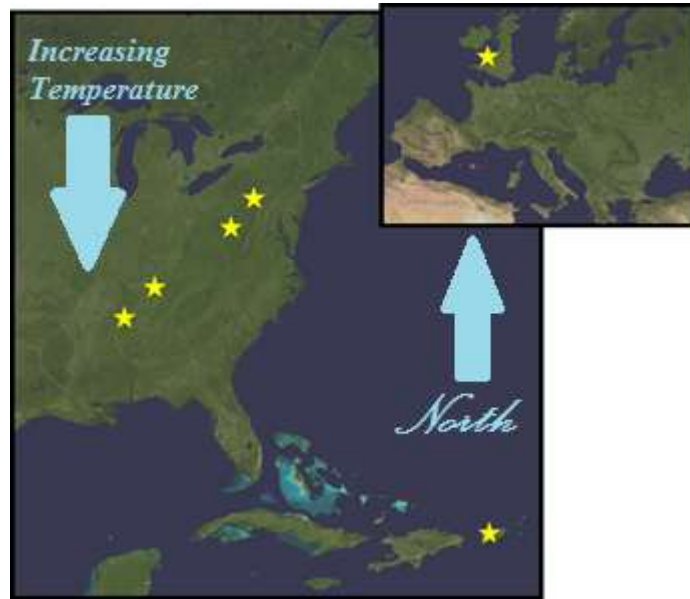


Figure 1a. Spatial map of sampling locations for the study.

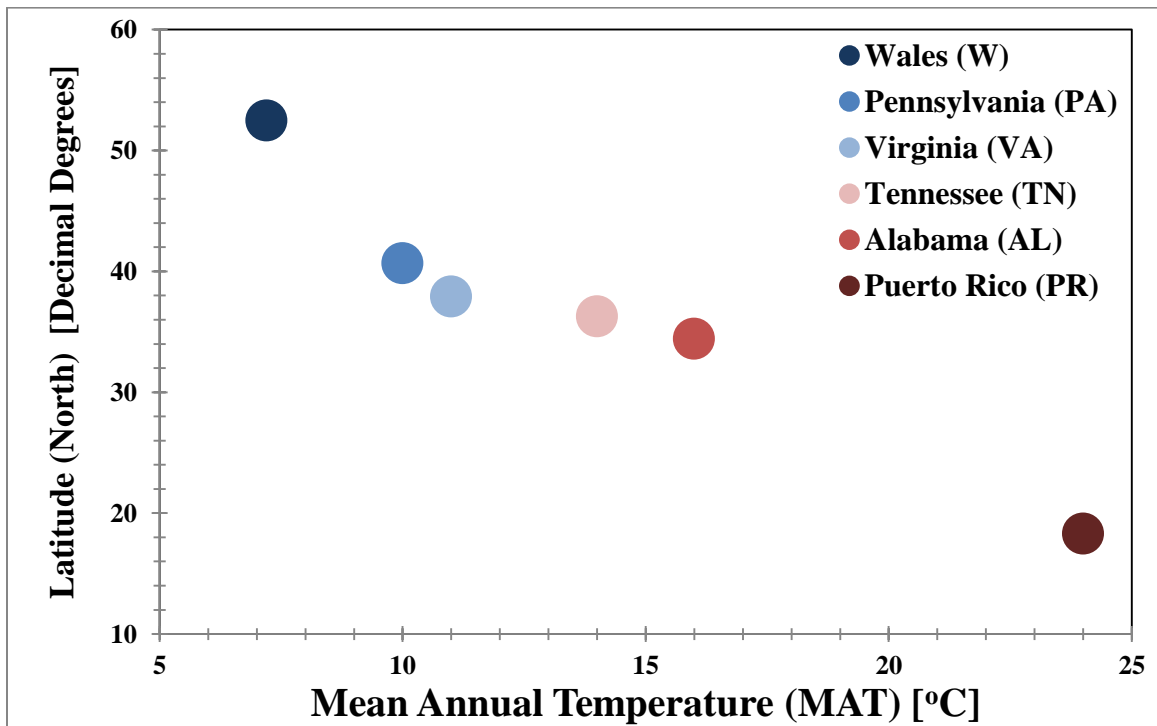


Figure 1b. Latitude in decimal degrees plotted against MAT in °C. All latitudes are north of the equator. Sample site MAT increases as latitude decreases.

The sites were all chosen as ridgetop sites because these locations can be modeled as one dimensional water flow systems. All sites have similar underlying geology (iron-rich, organic

poor shale) and are located in relatively undisturbed forested areas (PA site has been cleared due to logging 2-3 times since the 1700's and PR has been fallow farming land for 40 years). Table 1 provides a detailed list of site information for each sample site (Dere et al. 2013)

Table 1. Soil sample site characteristics

Site	Latitude	Longitude	Elevation [m]	Relief [m]	Slope [o]	MAT [°C]	MAP [cm]	depth [cm]
Wales	N52° 28.416	W3° 41.575	417	87	0.29	7.2	250	35
Pennsylvania	N40° 39.931	W77° 54.297	297	40	0.1	10	107	28
Virginia	N37° 55.625	W79° 32.799	752	220	0.34	11	106	80
Tennessee	N36° 16.414	W83° 54.809	418	71	0.3	14	138	398
Alabama	N34° 25.375	W86° 12.400	241	43	0.35	16	136	220
Puerto Rico	N18 18.050	W66 54.401	366	25	0.16	24	234	613

Soil and rock samples were collected previous to this study as outlined in Dere et al. (2013). Soil samples were collected by hand augering to the depth of refusal, or the point at which a hand auger cannot be driven further (Dere et al. 2013). Soil samples were collected in ~10 cm intervals to refusal. Additionally, soil pits were dug at most of the sites and physical properties were described (Soil Survey Staff 1993). Figures 19-24 show the identified horizon names for most soil sample locations. In TN, AL and PR, hand augering was continued from the bottom of the soil pit until refusal. The profiles vary greatly in depth between 28 cm (PA) and 632 cm (PR).

Rock samples used as parent material for the overlying soils were collected from exposed outcrops near the ridges. Soil samples and rock fragment samples were taken from the bottom of

soil pits (if fragments were present). These outcrop locations were taken after careful consideration of stratigraphy and their proximity to the sampling locations.

2.2 Sample Analyses

Bulk soil samples (all size fractions) were air-dried, crushed, and ground. After grinding, samples were split with a riffle soil splitter four times. Rock and soil samples were then completely ground by hand using a mortar and pestle to <149 microns (100 mesh). This bulk sample was then analyzed for all sites.

Major elements were measured by inductively coupled plasma atomic emission spectroscopy on a Perkin-Elmer Optima 5300DV Inductively Coupled Plasma-Atomic Emission Spectroscopy (ICP-AES) (Penn State Materials Characterization Lab (PSU-MCL), Senior Analyst Henry Gong). Following the process outlined by Medlin et al, (1969), samples were prepared for ICP-AES by fusing 100 mg of the ground sample with 1 g of lithium metaborate at 950 °C and then promptly dissolving the fused sample in a 5% nitric acid solution for 30 minutes (Medlin et al. 1969).

Total carbon and total nitrogen were measured on a CE Instruments Elemental Analyzer EA 1110 with a thermal conductivity detector (Soil Research Cluster Lab PSU). Between 13-18 mg of samples were weighed and loaded into tin vials for combustion using a combination of two precision scales. One reference sample was run twice before our samples and every 10 samples a duplicate was run to ensure reproducibility of the data.

2.3 Preliminary Data Processing

Soil bulk density, ρ_b [g cm^{-3}] was used in many of the preliminary data calculations; our bulk densities were calculated using the equation outlined in Dere et al. (2013) and reproduced below as equation 1. Equation 1 shows that bulk density can be accurately estimated for any sample from any depth using a value for the maximum reasonable bulk density, b [g cm^{-3}], a surface bulk

density, ρ_b^o [g cm⁻³], a fit parameter related to the slope, K, and the depth of the soil sample, z [cm] (Dere et al. 2013)

$$\rho_b = \rho_b^o + \frac{(\rho_b^{max} - \rho_b^o)Kz}{1-Kz} \quad (1).$$

The mass transfer coefficient, τ [unitless], is used to show relative addition or depletion of an element with respect to an immobile element after normalization with respect to the concentration of an immobile element in the parent material (Brimhall and Dietrich 1987; Anderson et al. 2002). Equation 2 defines τ where $C_{j,w}$ [wt. %] is the concentration of mobile element j in the weathered sample, $C_{j,p}$ [wt. %] is the concentration of j in the parent material, $C_{i,w}$ [wt. %] is the concentration of immobile element, i, in the weathered sample and $C_{i,p}$ [wt. %] is the immobile element concentration in the parent material

$$\tau = \frac{C_{j,w}C_{i,p}}{C_{j,p}C_{i,w}} - 1 \quad (2).$$

The elemental composition of parent material was determined by averaging elemental concentrations from the collected rock samples. The immobile element used for τ calculations for soils from W, PA, TN, AL and PR was Zr. However, the soil from Virginia exhibited Zr concentrations 3-5x larger than the concentration in the samples used for VA parent material. Thus, we could not use Zr as the immobile element at this site. Dere et al. (2013) argued that the sandstone stratigraphically above the shale is the source of the excess Zr, enriching the soil during weathering. Presently, the sandstone has been completely weathered away but has left residual Zr in the shale soil (Dere et al. 2013). Therefore we followed Dere et al. (2013) and used the Ti concentration for the VA soil after correcting for Ti losses. Equation 3 describes the correction we used for the Ti concentration:

$$C_{Ti,corrected} = C_{Ti,actual} + (\tau_{Zr,Ti}^{TN} + C_{Ti,actual}) \quad (3).$$

($C_{Ti,corrected}$ [wt. %]) used in the τ calculations for Virginia as described by Dere et al (2013) and Jin et al. (2010). It is assumed that Ti in VA is lost in similar proportions to the Ti in TN at the same depth scale (Dere et al. 2013; Jin et al. 2010)

Calculation of total C, N or Mn in a profile was also completed to assess integrated concentrations for those elements. Two methods were used. The first is a simple summation of concentrations at each sampling interval to calculate M_j [g cm^{-2}] as shown in equation 4 (Brimhall and Dietrich 1987):

$$M_j = \sum C_j \rho_w dz \quad (4).$$

Here, $C_{j,w}$ [wt. %], is the concentration of element j, ρ_w [g cm^{-3}], is the bulk density of the soil at depth z, and dz [cm] is the depth interval. The second method integrates τ values which have been corrected for soil strain over depth, producing net additions or depletions of an element with respect to the parent material (Brimhall and Dietrich 1987; Anderson et al. 2002; Brantley and Lebedeva 2011). The integrated mass outflux or influx, m_j [g cm^{-2}] is shown in equation 5:

$$m_j = C_{j,p} \rho_p \int_0^L \frac{\tau_j(z)}{\varepsilon(z)+1} dz \quad (5).$$

Although this is written as an integral, we calculated m_j by a summation of the values for each sampled depth interval. Here ρ_p is the density of the parent material, this is assumed to be a constant 2.64 [g cm^{-3}] which is an average for shales (Jin et al. 2010), L [cm] is the maximum depth of the profile, dz [cm] is the sample interval, $\tau_j(z)$ [unitless] is tau for element j at depth z and ε [unitless] is the soil strain for the soil interval. Soil strain is calculated using the equation originally derived by Brimhall and Dietrich (1987)

$$\varepsilon_i = \frac{\rho_p C_{i,p}}{\rho_w C_{i,w}} - 1 \quad (6).$$

2.4 Drivas et al. (2011) Model

Soil mixing via bioturbation, freeze/thaw, root-wedging, etc. can be most simply described by Brownian motion: a random diffusive motion of particles. Drivas et al. (2011) described the most basic model incorporating this process, the classic 1-D diffusive mixing equation (Drivas et al. 2011):

$$\frac{\partial c_j}{\partial t} = D_{eff} \frac{\partial^2 c_j}{\partial z^2} \quad (7).$$

The equation was solved analytically by Drivas et al. (2011) assuming steady-state; i.e., the concentration of element j no longer changes in time. The variables z and t are soil depth [cm] and time [years], respectively. C_j is the concentration of the element at any depth interval [g cm^{-3}]. D_{eff} is the diffusive mixing coefficient; which describes the magnitude of soil mixing occurring per year [$\text{cm}^2 \text{yr}^{-1}$]. Surficial deposition of element C_j (simulating leaf litter input for C and N or atmospheric deposition of Mn-sorbed particles) provides the only source of input for element C_j . Equation 7 was solved with two different assumptions with respect to surficial input: either a continuous surface deposition or a one time, extended interval of surface elemental deposition.

It is well known that C and N are constantly deposited to the surficial horizons of a soil profile via litter decomposition and root inputs, thus a continual surface input was used here to apply the Drivas et al. model for those elements. The steady-state solution for equation (7) from Drivas et al. for the assumption of a continuous surficial input is described as (Drivas et al. 2011):

$$C_s(z, t) = \frac{2Q}{D_{eff}} \left[\sqrt{\frac{(D_{eff})(t)}{\pi}} \exp\left(\frac{-z^2}{4(D_{eff})(t)}\right) - \frac{z}{2} \operatorname{erfc}\left(\frac{z}{2\sqrt{(D_{eff})(t)}}\right) \right] \quad (8).$$

In equation 8, Q is the continuous surface deposition rate of element j per unit area [$\text{gyr}^{-1} \text{cm}^{-2}$], *exp* is the exponential function and *erfc* is the complementary error function.

In contrast to C and N, Mn is deposited mainly via atmospheric deposition. For example, one researcher has concluded that most Mn in the northeast was deposited in soils as Mn sorbed to dust (Herndon et al. 2011). Accordingly, much of the Mn deposition in Eastern U.S. soils occurred over a period of ~70 years during the last century until the Clean Air Act significantly

cut emissions (Herndon and Brantley 2011). To represent this period of deposition, the model was solved with a timed deposition of 70 years during a 100 year run. Equation 9 represents the steady-state solution for this model as presented originally by Drivas et al. (2011):

$$C_s(z, t) = \frac{Qz}{Def f} \left[\sqrt{\frac{\exp(s_L^2)}{\sqrt{\pi}s_L} + \operatorname{erf}(s_L) - \left(\frac{\exp(-s_U^2)}{\sqrt{\pi}s_U} \right) - \operatorname{erf}(S_U)} \right],$$

here, the following terms are defined:

$$s_L = \frac{z}{2} \sqrt{(Def f)(t)} \quad s_U = \frac{z}{2} \sqrt{(Def f)(t - T)} \quad (9).$$

All other terms are defined previously; however, it should be noted that t is the total time for the model run and T is the time of deposition and Q is the surface deposition during time T (Drivas et al. 2011).

3. Results

3.1 Concentration versus depth profiles

It is first prudent to gain knowledge of how the concentration profiles of C, N and Mn change with depth in order to gain insight into where the majority of the element is being stored in the soil profile. It is also necessary to have concentration profiles versus depth to compare with the modeled results. The profiles presented were cropped at 100 or 200 cm if necessary to show the concentration profile dynamics in more resolution. Full concentration profiles can be seen in Figures 19-24 in the Appendix.

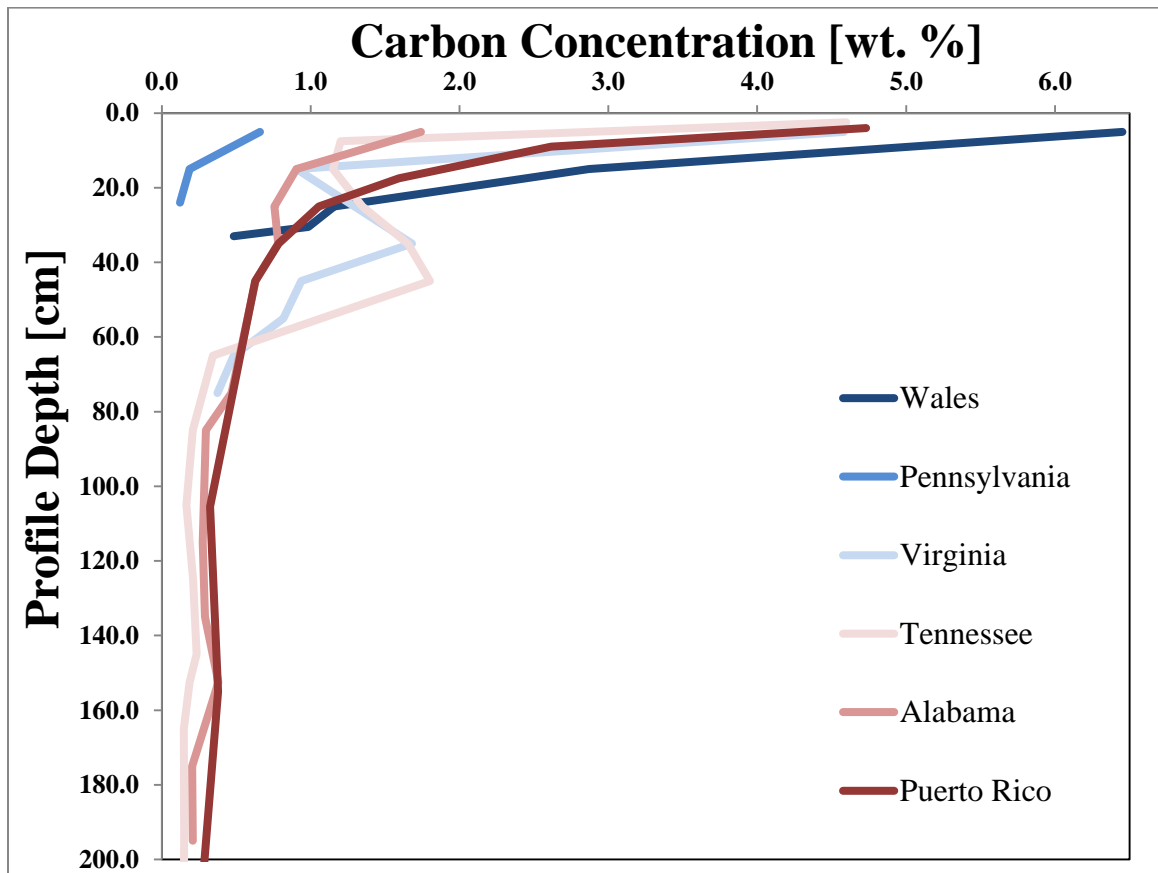


Figure 2. Carbon concentration versus depth for each sample site. The concentration profiles are plotted against profile depth to 200 cm. Only Puerto Rico and Tennessee extend further than 200 cm; however, the change in their concentrations at deeper depths is minimal compared to the concentrations at 200 cm. The colors change from dark blue (coolest climate, Wales) to dark red (warmest climate, Puerto Rico).

Wales has the most C on the surface, followed by Puerto Rico, Tennessee, Virginia, Alabama and finally Pennsylvania, with the least amount of C at the surface. In every soil the C and N concentrations generally decreased with depth (Figures 2 and 3). However, small increases in C were observed between 20 cm and 60 cm for Virginia (VA) and Tennessee (TN) in figure 2. This “bump” at depth was not seen in Wales (W), Pennsylvania (PA), Alabama (AL) or Puerto Rico (PR) in the same figure. The apex of the “bump” moves downward in depth with decreasing latitude (i.e., increasing MAT) between VA and TN.

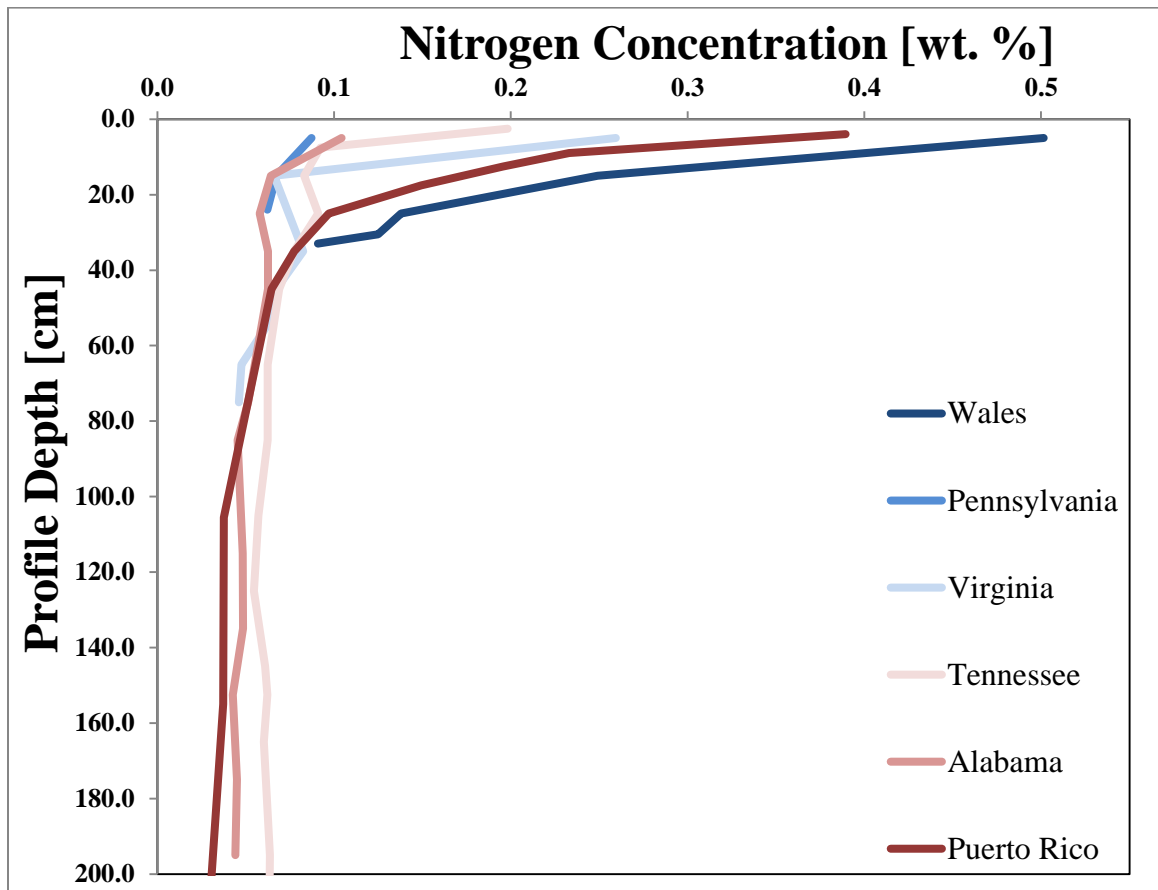


Figure 3. Nitrogen concentration versus profile depth for each sample site. Once again the sample locations are color coded for temperature (dark blue=coolest to dark red=hottest). The concentration profiles are also displayed against profile depth to 200 cm. Only Puerto Rico and Tennessee extend further than 200 cm; however, the change in their concentrations is minimal from the concentrations at 200 cm.

The “bumps” observed in the C profiles of VA and TN are also seen in the N profiles for these sites on a smaller scale (the increase at depth is less dramatic than in the C profile). At the surface, Wales has the highest concentration of N, followed by Puerto Rico, Tennessee, Virginia, Alabama and Pennsylvania. Overall, these profiles mimic the C profile shapes; however, the concentration is approximately one order of magnitude smaller.

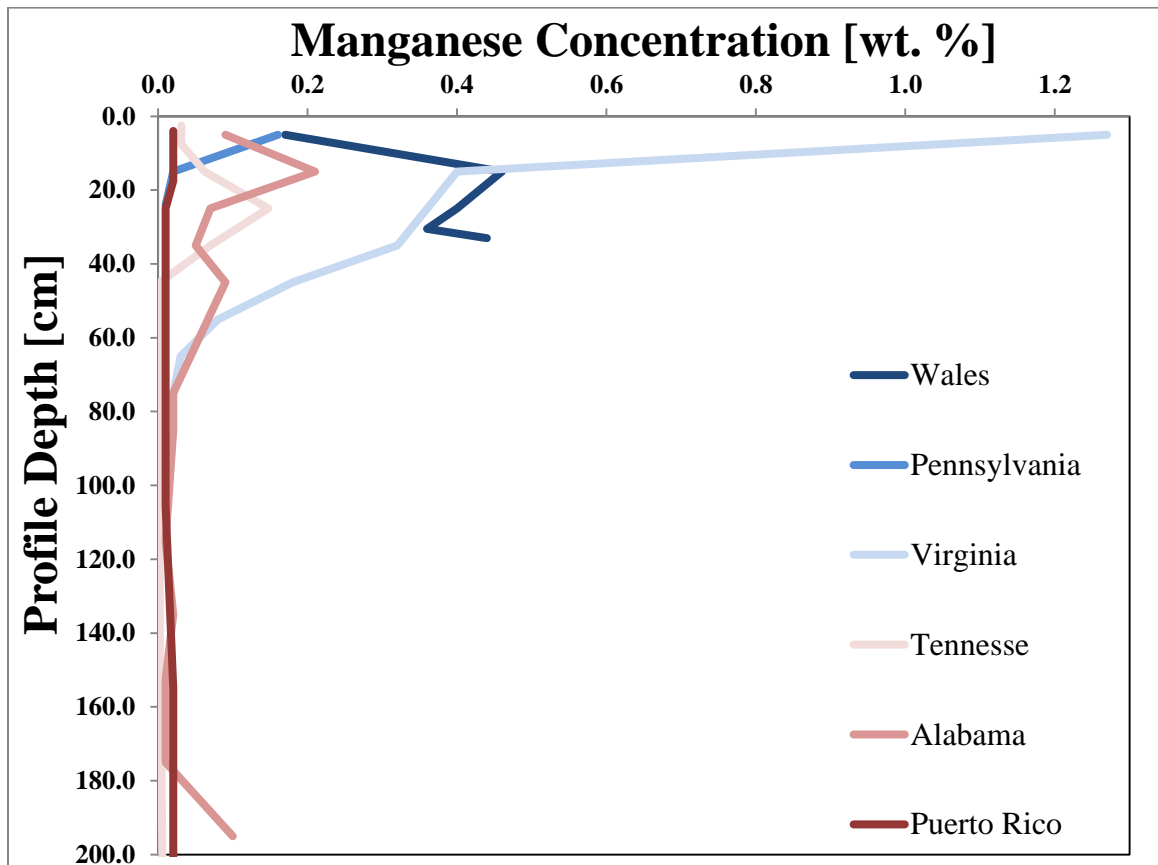


Figure 4. Manganese concentration versus profile depth. The samples sites are similarly color coded for increasing MAT, dark blue-coolest climate to dark red-warmest climate. The concentration profiles are displayed against profile depth to 200 cm. Only Puerto Rico and Tennessee extend further than 200 cm; however, the change in their concentrations is minimal from the concentrations at 200 cm.

Unless enriched from the parent material, generally Mn is not present in large quantities in the soils shown in Figure 4. Virginia has high Mn concentrations compared to all other sites: just over 1.2 weight percent compared to all other values which were less than 0.2 weight percent. In Wales, the profile shape is similar to the shape of the Tennessee and Alabama profiles with increasing concentrations at depth (around 20-30 cm). Pennsylvania shows a small enrichment towards the surface.

3.2 Tau Plots

The Drivas et al. model works only for profiles which show net enrichment at the surface, or true addition profiles. The mass transfer coefficient, τ , allows us to check the sampled profiles.

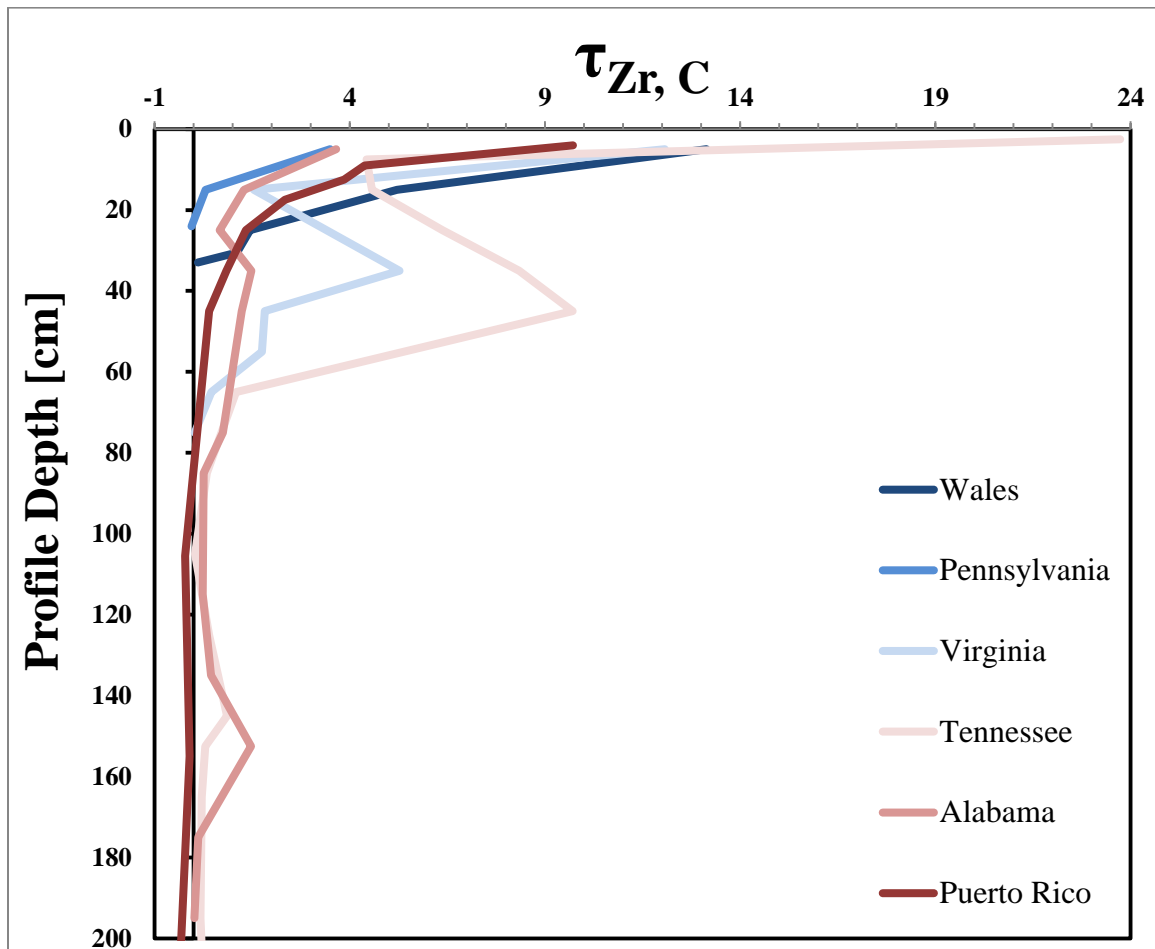


Figure 5. Mass Transfer Coefficient for carbon at all sites plotted versus depth. Parent material was assumed to equal the C concentration of the deepest soil sample for the full profile or an average of the 2 deepest soil samples' C concentration for each full profile. Wales, Virginia, Tennessee, Alabama and Puerto Rico used an average of the two deepest soil sample C concentrations. Pennsylvania used only the bottommost soil sample C concentration because the profile was so shallow. Zirconium is the immobile element for Wales, PA, TN, AL and PR sites. A corrected titanium concentration was used for the immobile element for VA.

All of the locations show positive τ values of C; these are all addition profiles. An increase in C between 20 and 60 cm is once again visible in the VA and TN τ profiles. Puerto Rico appears to be slightly depleted below 100 cm. Tennessee shows the most surficial enrichment ($\tau = 23.74$ for depth 0-1 cm) and Pennsylvania shows the least surficial enrichment ($\tau = 3.49$ for depth 0-10 cm). It is interesting to note that Wales, which had the highest weight % for C at the surface, is second to Tennessee when comparing τ values.

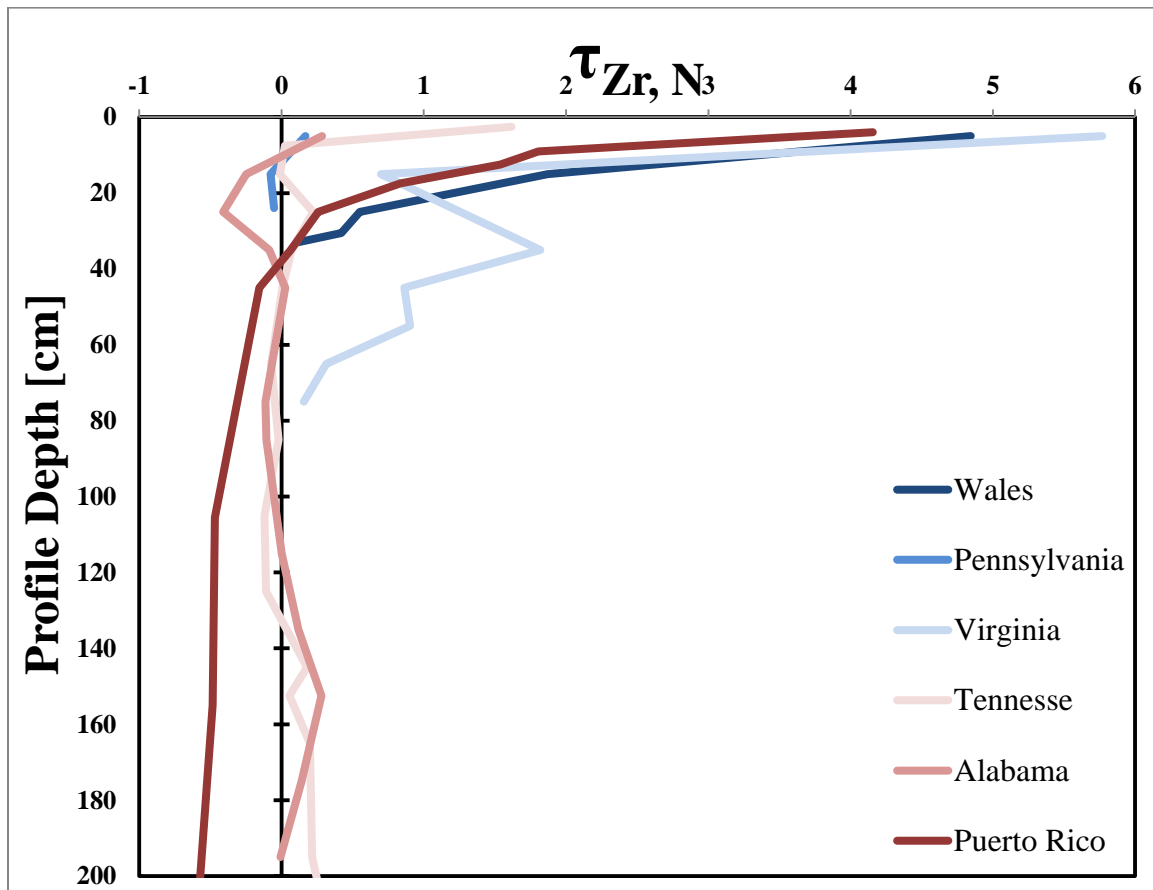


Figure 6. Mass transfer coefficient, τ , for nitrogen plotted versus depth at every site. Parent materials for all elements are exactly the same for the C τ plot (figure 5). Zirconium is the immobile element for Wales, PA, TN, AL and PR sites. A corrected titanium concentration was used for the immobile element for VA.

All sites are enriched at the surface with N; however, Alabama shows depletion just below the surface around 10 cm and then hovers around 0 throughout the rest of the profile. Tennessee returns to 0 net enrichment or depletions and also hovers around 0 to its basal layer of soil. It should be noted that TN does show a small increase in N around 20-30 cm that was also observed in the weight percent versus profile depth (Figures 2 and 3). The N profile shape for Virginia is similar to the C profile for Virginia; the “bump” in C around 40 cm is replicated in the N profile at 40 cm as well. Puerto Rico becomes depleted at 40 cm and stays depleted with depth. Wales is enriched at all depths. Pennsylvania is enriched to depths of 15 cm, where N becomes depleted at all deeper depths.

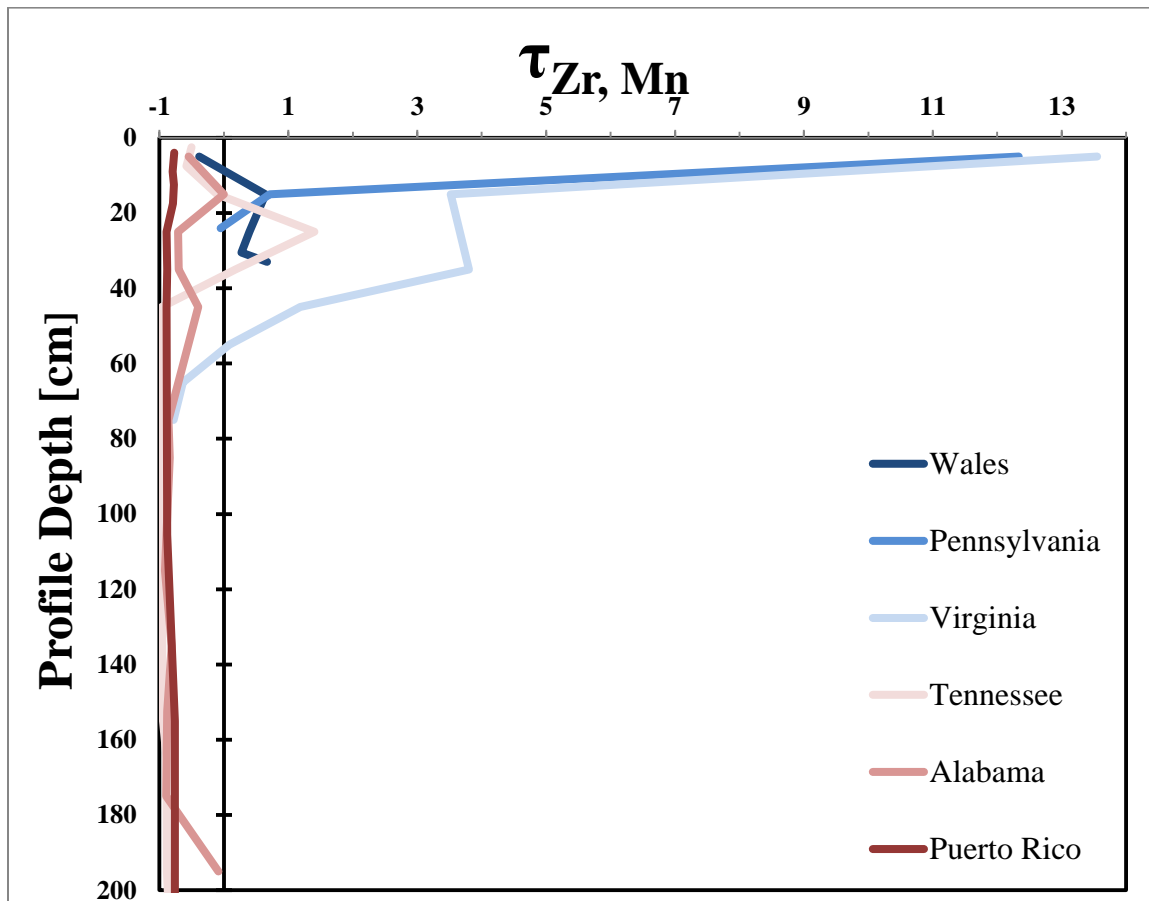


Figure 7. Mass transfer coefficient, τ , for manganese plotted against depth. Parent material is the same parent material used for τ plots of C and N (figures 5 and 6). Zirconium is the immobile element for Wales, PA, TN, AL and PR sites. A corrected titanium concentration was used for the immobile element for VA.

The only sites which show a characteristic addition profile for Mn are Pennsylvania and Virginia. Puerto Rico and Alabama have profiles which are always depleted and relatively constant in the fractional depletion values. Wales becomes enriched at depth, whereas it starts out depleted. Tennessee only shows enrichment between 20 and 40 cm; otherwise the soil is depleted of Mn.

3.3 M_j and m_j trends with MAT

To determine the total C, N and Mn in each profile we used two different summation methods: M_j , which includes the parent material and m_j , which excludes the parent material and accounts for soil strain. These concentration totals are compared to MAT to determine if trends

exist between the size of our element pools (total concentration for the whole soil profile) and temperature.

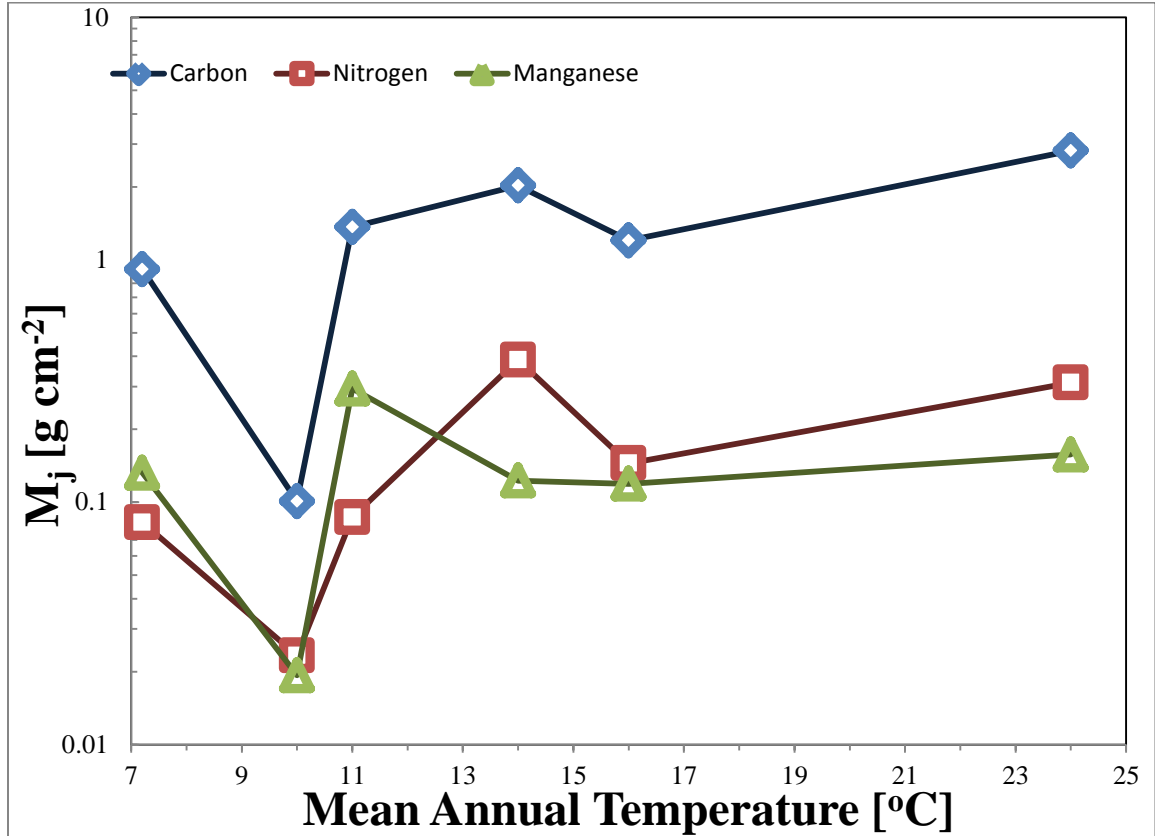


Figure 8. M_j for each element versus mean annual temperature (MAT). M_j is a simple summation of the total concentration in each sample for a soil profile. This total includes input from parent material.

The total concentration of C, N and Mn (M_j) in the soil includes any additions from the parent material. We see that, with the exception of PA, there is a general increase in M_j for $j = C, N$ and Mn between Wales and Puerto Rico. Wales and Virginia are the only two sites which show more total Mn than N in the soils. A significant decrease in C, N and Mn concentrations compared to all other sample locations is observed in Pennsylvania.

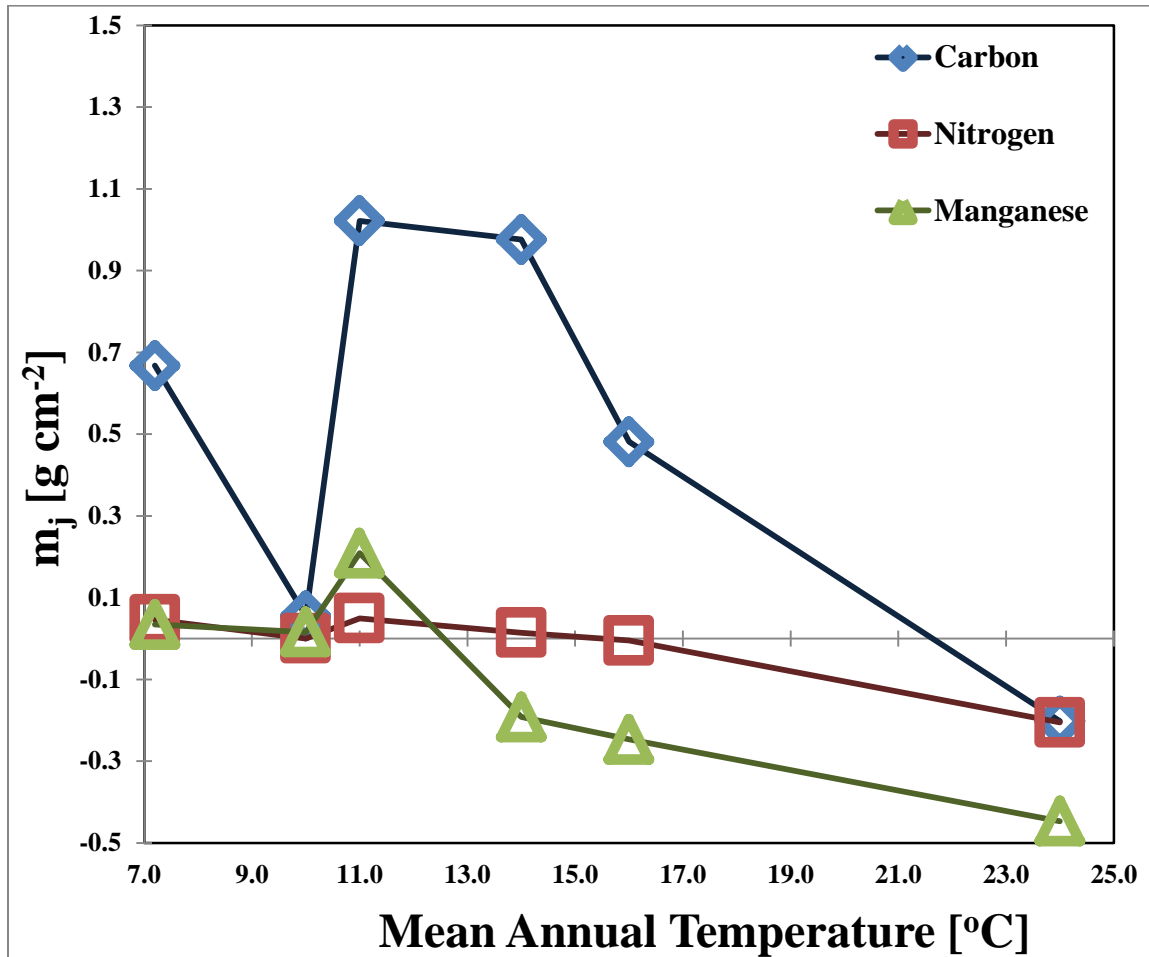


Figure 9. Plots of m_j versus mean annual temperature (MAT). “ m_j ” in this case refers to a summation of element concentrations that excludes input from parent material; it shows net addition or depletion of an element in the soil profile.

The integrated mass flux (m_j) shows the net additions or depletions of a soil profile which have been adjusted for strain. For all elements, an increasing then decreasing enrichment to eventual depletion by the warm end-member of the climosequence is observed as a general trend. The break point for increasing net mass and decreasing net mass is between 11 and 14 °C (between VA and TN). Pennsylvania is the exception to this trend, showing a decrease in total additions of all elements but especially C. Compared to Figure 8 which shows Tennessee, Alabama and Puerto Rico with significant accumulations of C, N and Mn, the integrated mass

flux shows a decrease in additions compared to cooler sample locations. The only profile to show all net partial depletions for C, N and Mn is also the deepest and warmest (PR).

4. Discussion

4.1 C and N coupling in soils

Much of our study is aimed at discovering how and why C, N and Mn are stored in soil in the manners we observed. C:N ratios can tell us how two of our elements change with respect to each other; providing insight into potential causes for profile shape variation. It is well known that the C:N ratio decreases as SOM decomposition increases (Booth et al. 2005). Carbon is used in the decomposition process and released from the soil as CO₂ while N is more likely to be mineralized by organisms and stored in the soil.

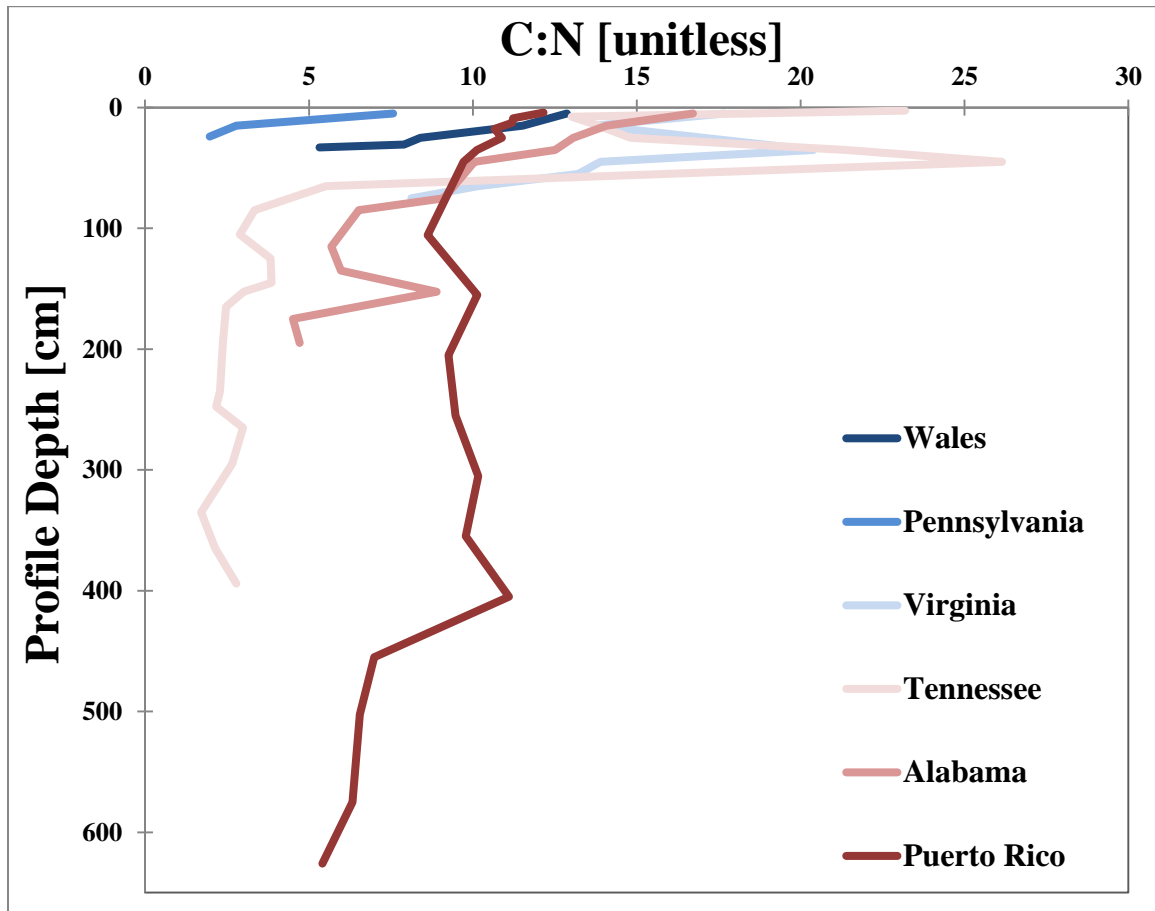


Figure 10. C:N ratio versus depth. C [wt. %] were divided by N [wt. %] and compared against depth. The sample sites are colored to represent the climate gradient (dark blue-coolest to dark red-warmest).

The surface soils for every sample site have the highest C:N ratios. However, at the VA and TN sites, the C:N ratio increases significantly between 30 and 50 cm compared to the rest of the profiles (C:N=20.39 and C:N=26.14 respectively). At greater depths, the TN profile appears to stabilize at a ratio of ~4. The observed decrease in the VA C:N ratio is similar to the TN profile at greater depths. Wales, PA and AL have generally decreasing C:N ratios with depth. The AL profile does show a small increase in the C:N ratio around 170 cm (C:N=8.89). Puerto Rico has a comparatively steady C:N ratio with depth. In a review by Booth et al. (2005), surface (top 10-15 cm) C:N ratios for upwards of 100 forested soils ranged between 8 and 58, with a median of approximately 25 (Booth et al. 2005). The surface soils in this study fall between these values. However, our median is lower than the median in the study by Booth et al (2005): ~15 compared to ~25.

The significant increases of C: N ratios at the VA and TN sites between 30 and 50 cm depth have two possible causes: SOM translocation and subsequent accumulation deeper in the profile or new SOM is being introduced via roots at depth. SOM translocation is prevented by increased clay in the soil. The horizon data in Figures 19-24 in the Appendix show that the first increased clay layer (Bt horizon) appears right around the same depth as increases in our element concentrations and C:N ratios appear. This would imply that the increased C: N ratios are due to the translocation of clays with adsorbed or occluded SOM from the surface and the subsequent accumulation of SOM in the Bt horizon. Small differences in the exact depths at which the Bt horizons first appear and the increases in C:N ratios and C & N concentrations are observed could be explained by the fact that the soil samples were sampled on 10 cm intervals without regard to horizonation.

4.2 Model fits

Model equations 8 and 9 based on the Drivas et al. (2011) study were fit to all of our profiles. Some fits were better than others (all element profiles for W, PA and PR were fit better than VA, TN and AL). Equations 8 and 9 were modified by adding a baseline concentration. This was done because we assumed there was a small background concentration of each element in the soil before the surficial input began. This baseline concentration was assumed to be the parent concentration of each element in the soil. The parent concentration of each element in this study was defined as the elemental concentrations in the deepest soil (PA) or an average between the two deepest soil samples (all other sampling locations). These parent concentrations are the same values used to create the τ plots (Figures 5-7).

The two fit parameters used in this model have different effects on the shape and magnitude of the concentration profiles produced. The net input rate determines the order of magnitude for the element's concentrations in the soil. Thus, it does not change the shape of the modeled profile as much as it increases or decreases (in concentration magnitude) the entire produced concentration profile. The net input includes both the surficial input of the elements to the soil over time but also (if applicable, i.e.: C & N) the removal of certain elements from the soil via decomposition. Therefore, the model will underestimate the actual input rate of C and N. However, the net rate will provide insight into the balance between true C & N input and decomposition (loss). The net input rate for Mn does not include decomposition; therefore, it is closer to the actual input rate of Mn.

The diffusional mixing coefficient, D_{eff} , is the parameter which predominantly controls the shape of the model. This value determines how much the soil is mixed over one year; this value is specific to a sample site, not the individual elements. Vertical mixing of the soil transports C, N and Mn downward through the profile. A small value of D_{eff} ($0-0.5 \text{ cm}^2\text{yr}^{-1}$) is consistent with a large concentration of C, N and Mn in the surface and a rapid decline with depth to the parent material concentration. Comparatively, a large D_{eff} value yields a profile that has more of the

surficial input distributed at depth. High surface concentrations are possible but there would also be higher concentrations than the parent material deeper in the profile.

Large absolute errors, which are sometimes observed in the model fits, are something that should only be of concern if the model is not following the same general shape of the profile. For simplicity, a fit was chosen if most of the data points and the model values were on the same order of magnitude and under 30% different. Often there are large absolute errors between the model and the deepest sample; these do not necessarily make for a poor model fit. For the cases of TN and PR, the concentration profiles were only modeled to 100 and 200 cm respectfully; at these depths the variability in concentrations of C, N and Mn is minimal. Thus, these sample concentrations are not the concentrations used for the calculation of parent material in the model (the absolute bottommost sample(s)). Therefore, the parent material concentrations used in the model will not match the concentrations at 100 or 200 cm (if the soil profile extends this deep) and absolute error may increase.

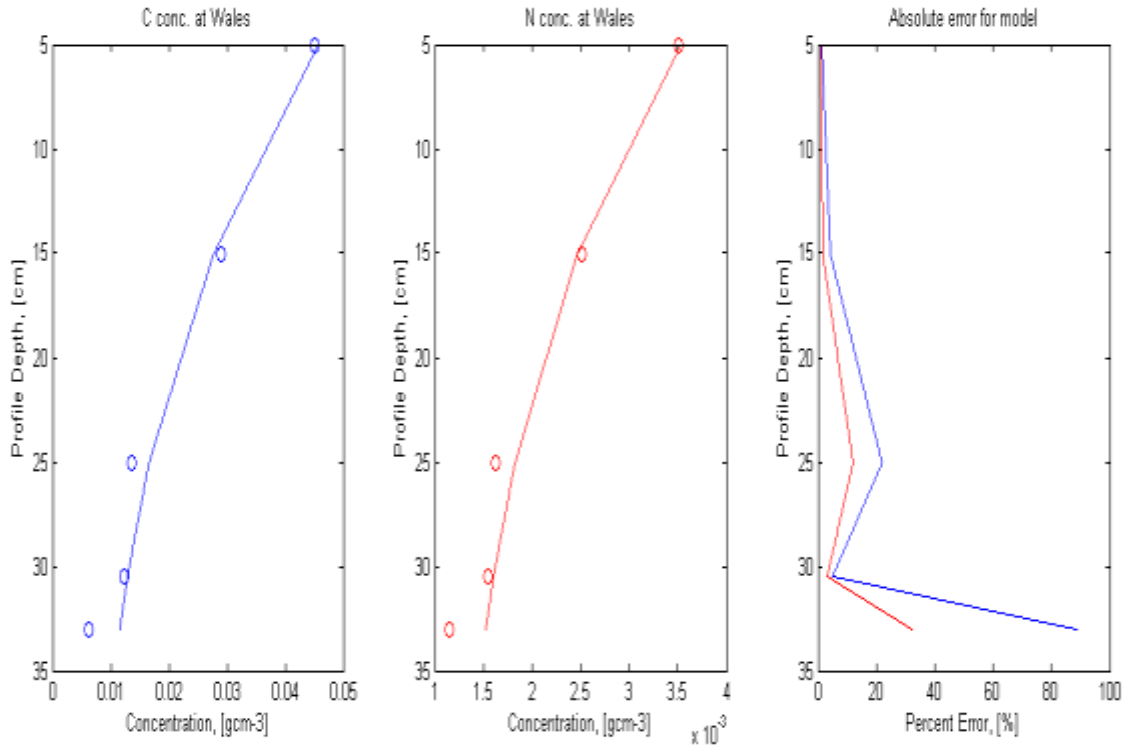


Figure 11. Model fits to carbon and nitrogen concentration in Wales and the absolute error vs. depth for the aforementioned model fits. $D_{\text{eff}} = 3.05 \text{ cm}^2 \text{ yr}^{-1}$, C input = $0.008 \text{ g cm}^{-2} \text{ yr}^{-1}$, C baseline = 0.0061 g cm^{-3} , N baseline = 0.0012 g cm^{-3} , N input = $0.000471 \text{ g cm}^{-2} \text{ yr}^{-1}$.

In Wales, the model fits the observed profiles with the exception at the lowest sample depth (32.5 cm). The model, run with this D_{eff} value, does not produce values at the baseline concentration at this depth; instead, it is still incorporating elemental input from the surface at the base of the profile. However, this particular D_{eff} value was chosen because it provided a good fit for all other sampled data higher than the bottommost sample compared to other, lower D_{eff} values. There was no reason to try to fit Mn for Wales because Mn was depleted at the surface (Figure 7) and the model is designed only for modeling addition profiles.

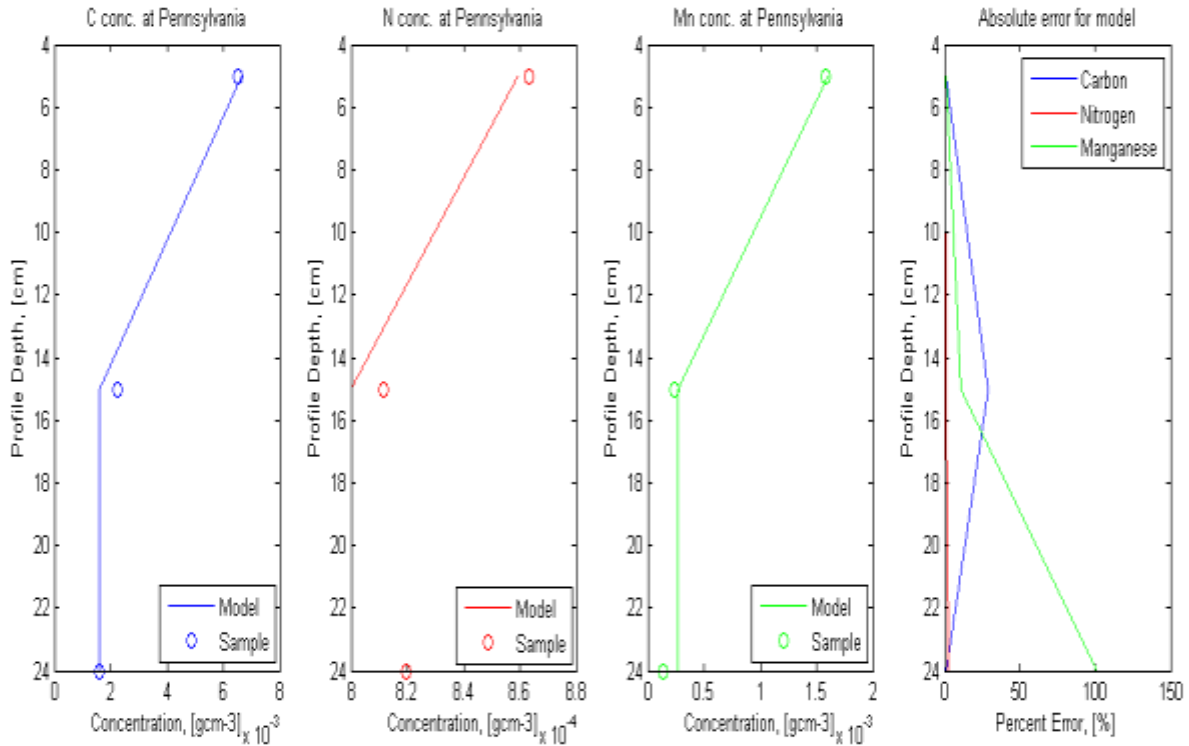


Figure 12. Model fits to carbon, nitrogen, manganese concentration profiles for Pennsylvania and the absolute error vs. depth for the aforementioned model fits. $D_{eff}=0.1\text{ cm}^2\text{yr}^{-1}$, C input= $0.0085\text{ gcm}^{-2}\text{yr}^{-1}$, C baseline= 0.0016 gcm^{-3} , N baseline= 0.0008 gcm^{-3} , N input= $0.00001\text{ gcm}^{-2}\text{yr}^{-1}$, Mn input= $0.00024\text{ gcm}^{-2}\text{yr}^{-2}$, Mn baseline= 0.000265 gcm^{-3} . Nitrogen is plotting exactly on the $8 \times 10^4\text{ [gcm}^{-3}]$, thus it is covered by the axis line.

Pennsylvania’s soil core showed an addition profile for C, N and Mn (Figures 5-7); thus, the model was used to fit all of these elements. In the process of fitting the model for PA, most attention was given to the Mn profile fit because the model does encompass Mn transport and assumes Mn immobility. The increased error at the bottommost sample for Mn does not detract from the quality of the model fit. The concentration calculated by the model at the lowest sample interval was 0.0003 gcm^{-3} and the concentration of the lowest sample is 0.0001 gcm^{-3} . These values are on the same order of magnitude (both 10^{-4}), but the concentration of the model is almost 3 times more than the surface sample.

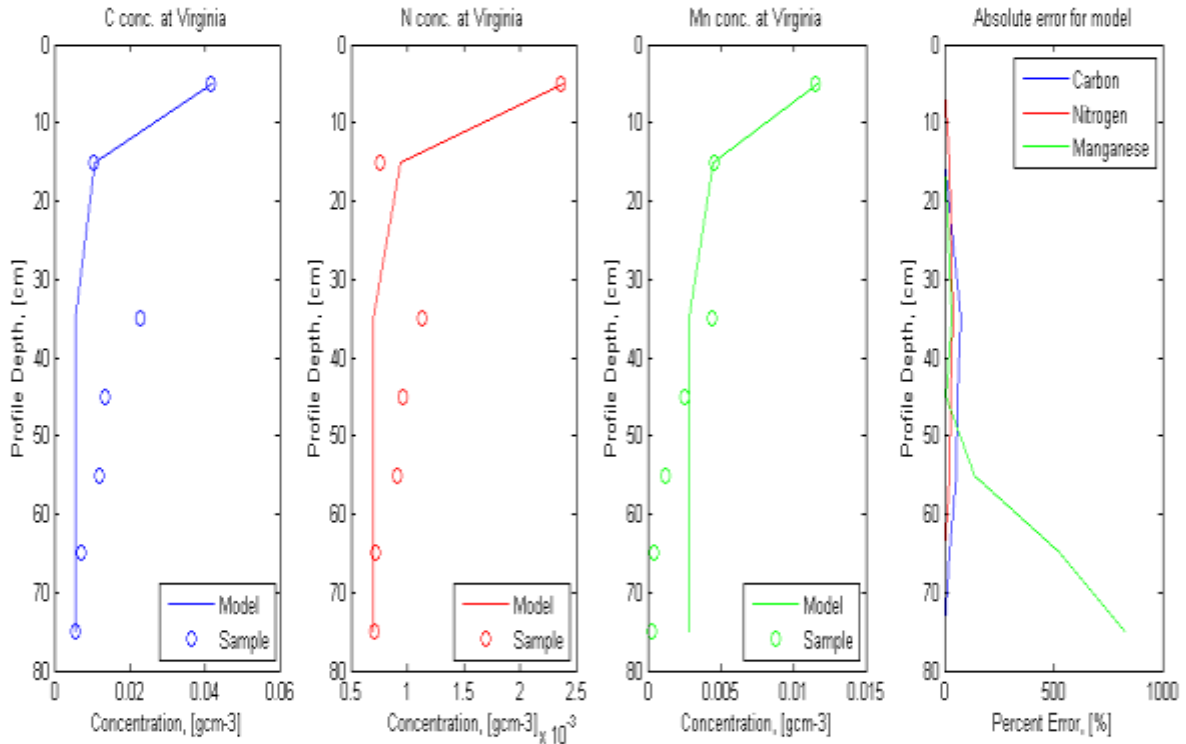


Figure 13. Model fits to carbon, nitrogen, manganese concentration profiles for Virginia and the absolute error vs. depth for the aforementioned model fits. $D_{\text{eff}} = 0.48 \text{ cm}^2 \text{ yr}^{-1}$, C input = $0.00457 \text{ gcm}^{-2} \text{ yr}^{-1}$, C baseline = 0.0057 gcm^{-3} , N baseline = 0.0007 gcm^{-3} , N input = $0.000212 \text{ gcm}^{-2} \text{ yr}^{-1}$, Mn input = $0.00152 \text{ gcm}^{-2} \text{ yr}^{-2}$, Mn baseline = $0.000283 \text{ gcm}^{-3}$.

At the Virginia site, C, N and Mn all showed addition profiles (Figures 5-7); thus, the model was used to fit all the elements. The model fits for Virginia are good. The average percent error for C and N are 30.2% and 16.5% respectively; however, there are basic failings in the model that are noticeable in Figure 13. As discussed previously, the C and N concentration profiles show an increase in concentration between 30 and 40 cm (the “bump”). As mentioned earlier, no term in the model can describe the processes producing the “bumps.” Additionally, the Mn profile becomes depleted after 55 cm (Figure 7) and once again the model cannot produce depletions of an element due to its simplicity; thus error is increased.

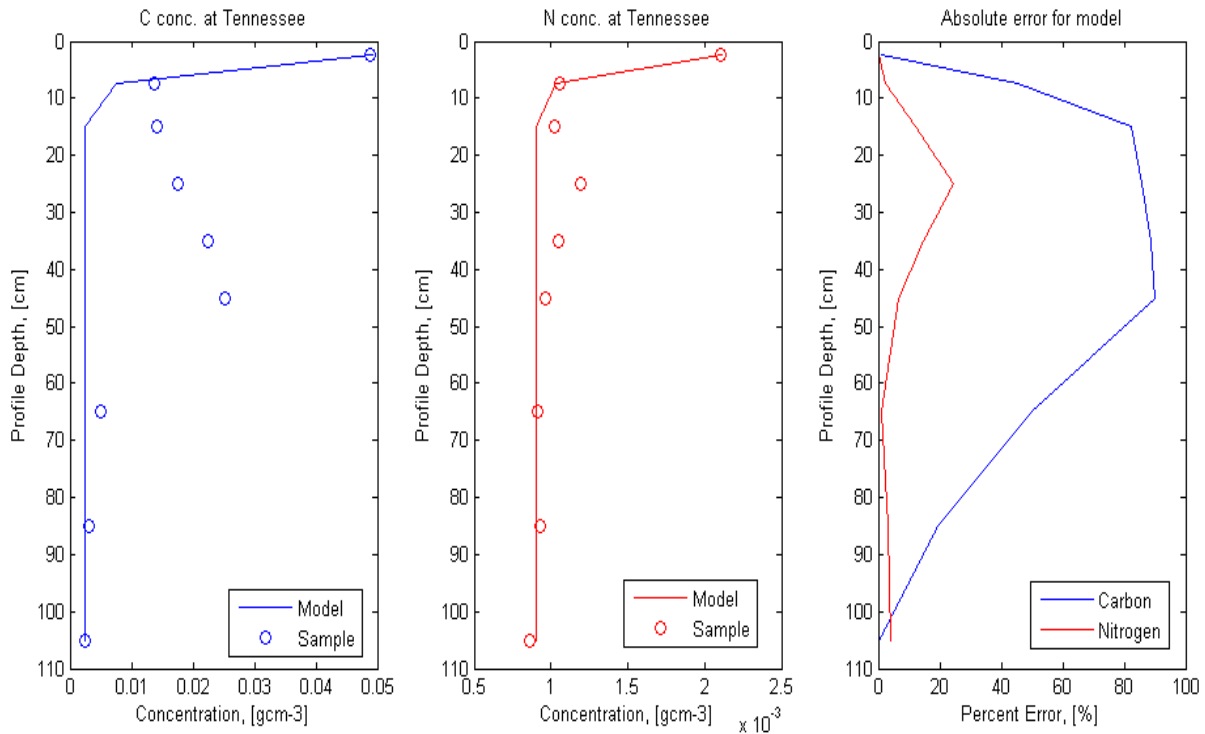


Figure 14. Model fits to carbon and nitrogen concentration in Tennessee and the absolute error vs. depth for the aforementioned model fits. $D_{eff}=0.1\text{ cm}^2\text{yr}^{-1}$, C input= $0.0029\text{ gcm}^{-2}\text{yr}^{-1}$, C baseline= 0.0025 gcm^{-3} , N baseline= 0.0009 gcm^{-3} , N input= $0.000075\text{ gcm}^{-2}\text{yr}^{-1}$. This profile was cropped at 105 cm; this is the depth at which fluctuations in concentration become minimal.

At the Tennessee sample location, the soil only showed addition profiles for C and N (Figures 5 & 6); thus, Mn was not modeled for TN. The fit for TN is relatively okay, with error due to the increased concentrations observed between 30 and 60 cm (the “bump”). Notice that the absolute error increases in the same range as the “bumps” seen in the C and N concentration profiles. The reason for the failure to fit is the same reason for the VA fit failures; the model is too simple to include processes which would produce concentration increases at depth.

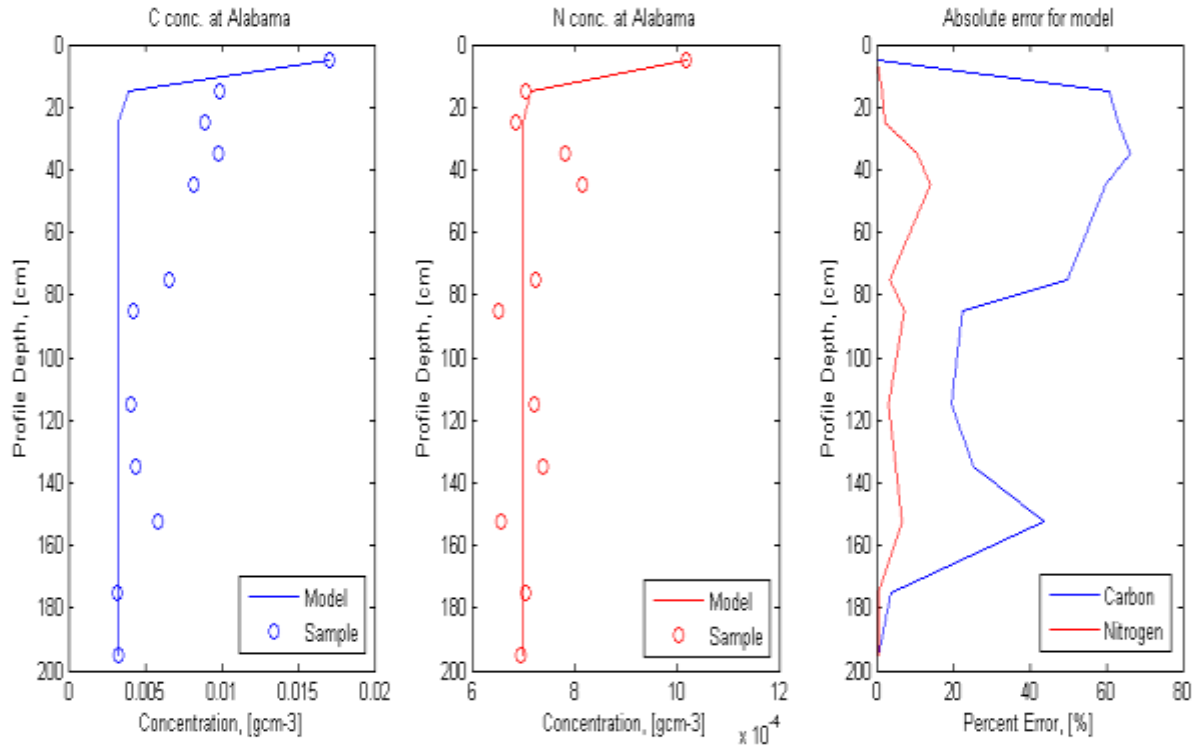


Figure 15. Model fits to carbon and nitrogen concentration in Alabama and the absolute error vs. depth for the aforementioned model fits. $D_{\text{eff}} = 0.25 \text{ cm}^2 \text{ yr}^{-1}$, C input = $0.00172 \text{ g cm}^{-2} \text{ yr}^{-1}$, C baseline = 0.0033 g cm^{-3} , N baseline = 0.0007 g cm^{-3} , N input = $0.00004 \text{ g cm}^{-2} \text{ yr}^{-1}$.

In the Alabama soil, C and N were once again the only elements to show addition profiles (Figures 5 & 6); thus, these were the only two elements modeled at this site. The average absolute error for C and N was 34.6 % and 4.5 %, respectively. The model fit for AL was okay for C; the model fails to fit the sample concentrations between 10 and 85 cm while simultaneously fitting surface samples and samples below 85 cm. Once again, there are processes occurring at depth that retain C and the model does not incorporate processes that would retain C in this manner. However, the average absolute error is low relative to the quality of fit in portions of the profile. Comparatively, the model does a good job portraying the N concentration profile at Alabama. The fluctuations observed in the profile are small compared to the concentration values ($\sim 0.0006 \text{ g cm}^{-3}$ compared to $\sim 0.0008 \text{ g cm}^{-3}$). This allows for a very small average absolute error and a good fit.

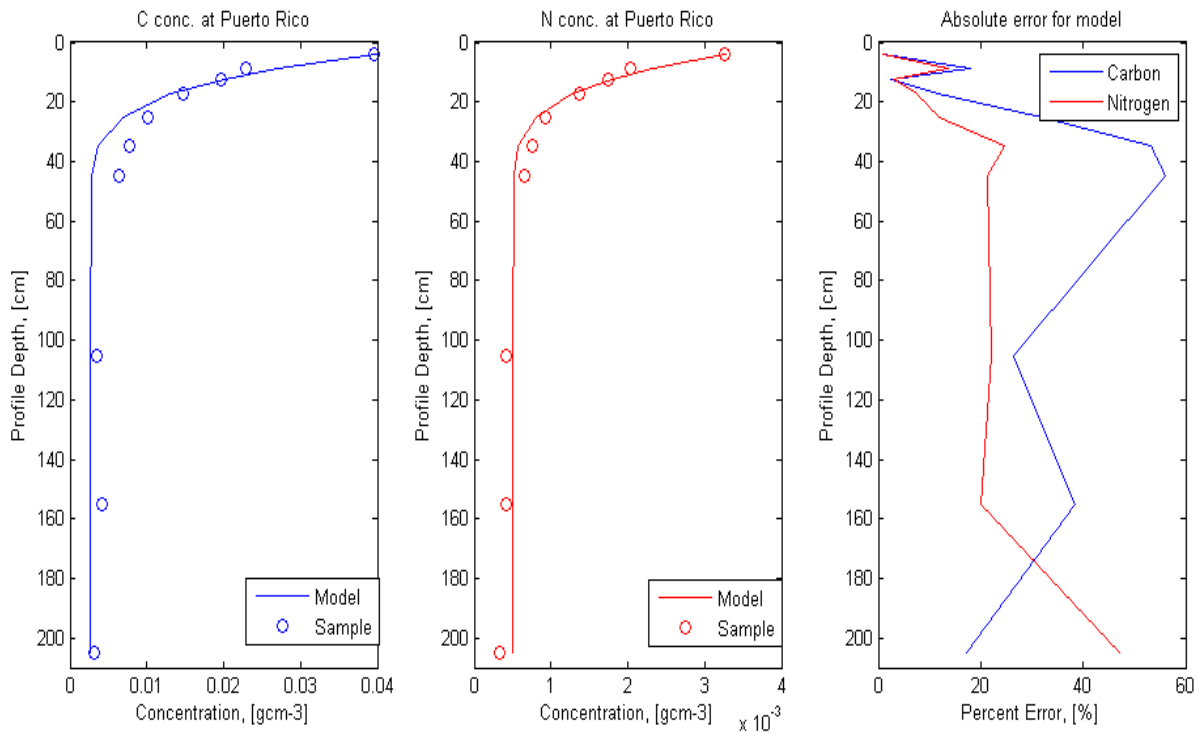


Figure 16. Model fits to carbon and nitrogen concentration in Puerto Rico and the absolute error vs. depth for the aforementioned model fits. $D_{er}=1.5\text{ cm}^2\text{yr}^{-1}$, C input= $0.0055\text{ gcm}^{-2}\text{yr}^{-1}$, C baseline= 0.0026 gcm^{-3} , N baseline= 0.0005 gcm^{-3} , N input= $0.00041\text{ gcm}^{-2}\text{yr}^{-1}$. The profile is cropped at 200 cm because the fluctuations in C and N were not significant deeper in the profile.

C and N were the only elements that showed addition profiles at Puerto Rico (Figures 5 & 6); thus, Mn was excluded from the modeling at this sample location. This model was fit by achieving the closest fit for the top three and the lowest three samples in the profile. Both of these fits are great; the average absolute error for the C and N fits were 25.6% and 17.2%, respectively.

4.3 Climate influence on model results

The goal of our research was to explain the trends seen between the net mass of C, N and Mn in the soil and climate (MAT). From Figure 9 we determined that the mass of C, N and Mn in the soil increases with increasing MAT until approximately 11 to 14 °C. From this point, the elements decrease in net mass until PR; where C, N and Mn are all depleted in some quantity from the soil. On a basic level, this could indicate that the rate of input for C and N is increasing at a lower rate than that of decomposition. The point at which the total mass of each element begins to decrease

with MAT is the latitude at which the rate of decomposition overtakes the rate of true input. To further explore this theory, we compare our fit parameters for each site against MAT to look for trends in the net deposition and soil mixing with climate.

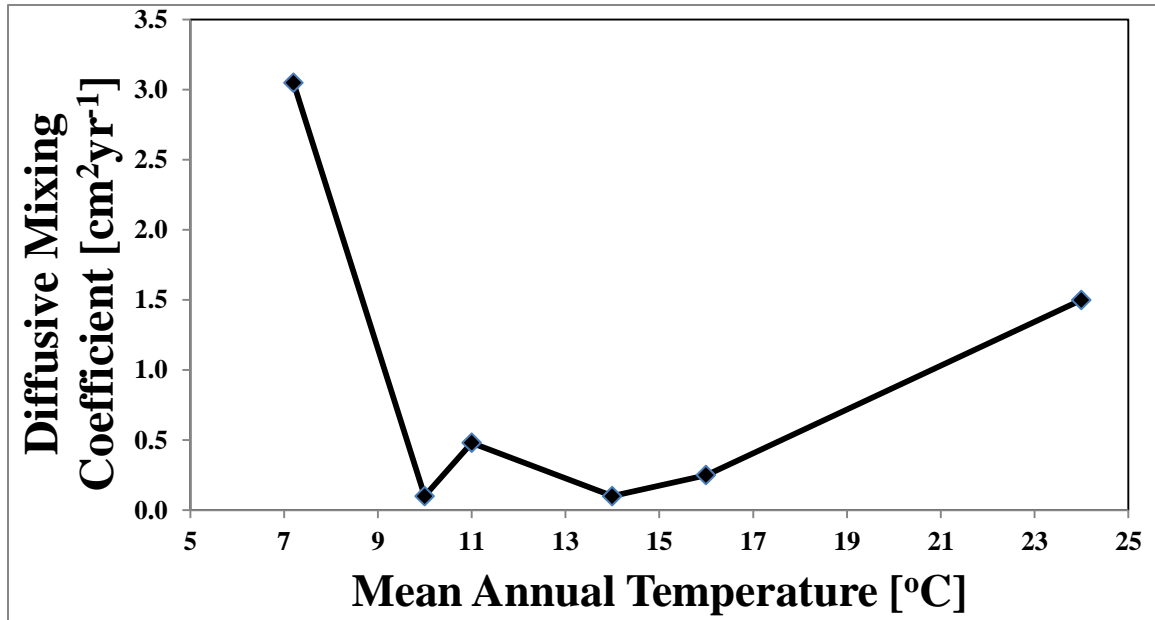


Figure 17. Diffusive mixing coefficients vs. mean annual temperature (MAT). The “ D_{eff} ” term from the model which describes how much soil is mixed over a year (diffusive mixing coefficient) was plotted against the MAT for each sample site. The D_{eff} term was the same for each element modeled per location.

The processes encompassed in the D_{eff} term can span many climates: frost-wedging, freeze-thaw, bioturbation and root growth (Kaste et al. 2007). Thus, we would not expect to see a clear trend with MAT and the D_{eff} values for each location. Figure 17 confirms this theory; the coldest and warmest end members have much higher D_{eff} values ($W=3.05 \text{ cm}^2\text{yr}^{-1}$ and $PR=1.5 \text{ cm}^2\text{yr}^{-1}$) than the Appalachian sites (average= $0.2325\pm 0.1555 \text{ cm}^2\text{yr}^{-1}$). Furthermore, there is a random variability to the D_{eff} values at the Appalachian sites. Despite the lack of trend between MAT and the soil mixing rate, there is a clear difference between sites of medium annual precipitation and high annual precipitation. Wales and Puerto Rico both receive approximately 250 cm (very wet) of precipitation per year while the Appalachian sites see about 120 cm (moderately wet) of

precipitation annually. The very wet sites have much larger soil mixing rates than the moderately wet sample locations.

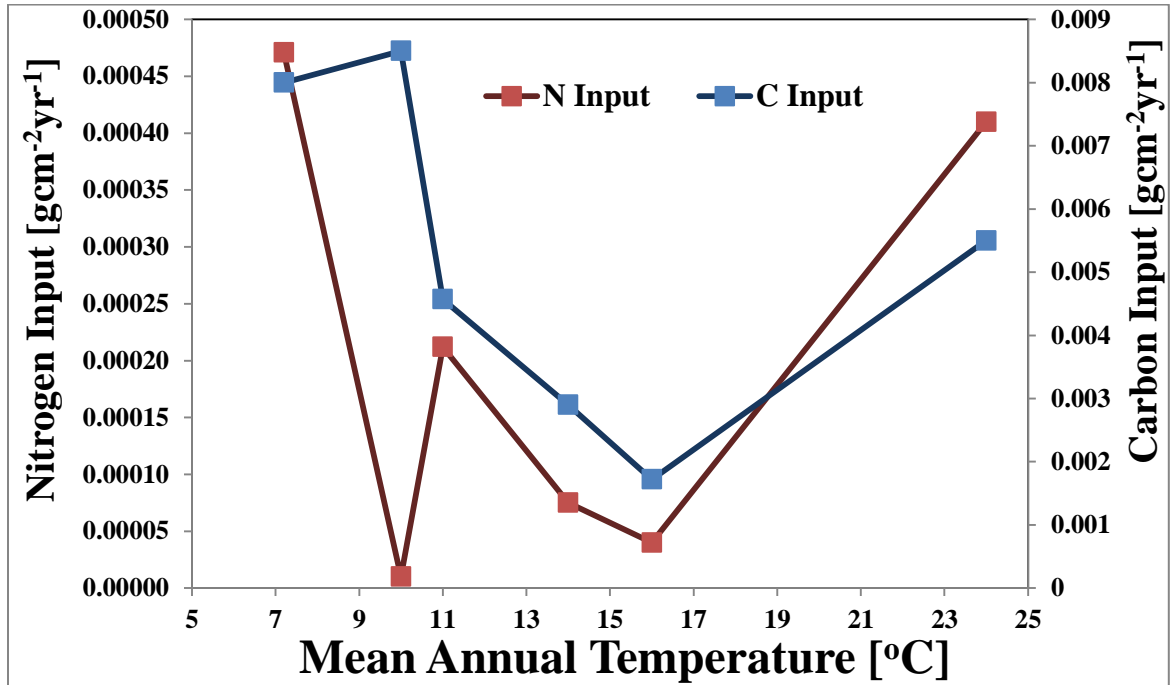


Figure 18. Carbon and nitrogen inputs derived from the models vs. MAT. Net carbon input is plotted against the right axis and net nitrogen input is plotted against the left axis.

The net input of C and N is decreasing with increasing MAT in Figure 18. This trend agrees with previous ideas about C and N dynamics in varying climates. It is known that C and N input to soil increases with increasing MAT. Also, decomposition of C and N in soil increases with increasing MAT (Jenny 1941). PR presents an exception to the observed trend. It is the warmest sample site, however it also has one of the highest net input rates (C input rate=0.0055 gcm⁻²yr⁻¹, N input rate=0.00041 gcm⁻²yr⁻¹). These elevated net input rates of C and N can be attributed to the increased precipitation in PR. Precipitation retards decomposition in the shallower soils; thus, the input rates observed for PR are closer to true C and N input rates (sans decomposition). The PR profile is still significantly depleted with C, N and Mn (Figure 9); which could be a product of the extreme depth of the soil profile. C and N surficial input will be decomposed before it can percolate to 6+ meters. Thus, deep soils (below 80 cm) in PR are still depleted with respect to the

parent material (Figure 5 & 6). The decline of net C and N input with increasing MAT coupled with the net mass trends seen in Figure 9 are suggestive of the theory that the rates of C & N input are increasing slower than the rates of C & N decomposition.

Finally, Mn was only modeled for PA and VA because these were the only two locations which indicated net Mn enrichment in the soil (Figure 7). The model does a good job at describing Mn distribution in soils (Figures 12 & 13). Mn does not show a trend with MAT or precipitation because its deposition to soils is attributed to pollution from iron refineries and steel production industries (point source). PA and VA are located in the areas which have been previously associated with these types of industry (Herndon et al. 2011). Therefore, it makes sense that these soils are enriched with Mn but not the other sample sites.

4.4 Error Discussion

4.4.1 Analytical Error

Error associated with the measured values of C, N and Mn in the soil was small. Reference samples for C and N analysis were measured with a calculated error of ± 0.005 mg and samples for analyses were measured with a calculated error of ± 0.05 mg.

The CHNS-O Elemental Analyzer reported an error of $\pm 0.5\%$ C and $\pm 0.1\%$ for N by reference samples and repeated samples. The limit of detection on the ICP-AES for Mn analysis was 0.005 weight percent and the error is close to $\pm 3\%$ of the recorded value.

4.4.2 Model Error

The model by Drivas et al. is simple in its design which has advantages (fast and easy application) but also disadvantages (misses major processes which could be affecting the results). The most egregious error in the model is that it excludes an explicit C and N decomposition term. The decomposition of C and N, which is accomplished via microbial action, results in the loss of C and N from the soil over time. What this means is that the model will underestimate the true

surficial input rate of C and N. Instead, the model implies a net input of C and N, from which relative trends in true input and decomposition can be deduced.

Decomposition of organic matter will also alter the shape of the profile; large decomposition rates will decrease the amount of surficial C or N that is found deeper in the profile. The lack of this term may artificially deflate the soil mixing coefficient term (D_{eff}). Consequently, some of the soils could have higher D_{eff} values than what the models currently portray. Despite these disadvantages, this model provides a good general picture of what is happening in these soils. I believe that it provides a more accurate picture of Mn than C or N because of the simpler nature of Mn in soils when assuming Mn immobility. To ensure accurate quantification of all soil processes affecting these elements and to better analyze element storage trends with climate, a more complicated model will be necessary.

5. Conclusions

C, N and Mn all have the potential to appear as addition profiles in soil; indicating net enrichment of these elements at the surface relative to the parent material (Figures 5-7). These addition profile-forming elements can be used to track soil processes and understand how these soil processes fluctuate with climate. The goal of this study was to use the simplest mathematical model possible to analyze how the net added or lost masses of C, N and Mn in soil changes with climate. We used the model by Drivas et al. (2011) to fit concentration profiles from a transect of sites which form a climosequence (Figures 11-16). An increase in net added mass of C, N and Mn was observed until 11-14 °C (between VA and TN). Then C, N and Mn decreased in net added mass to the warmest end member site (PR). PR showed partial net depletions for all three elements. The Drivas et al. model allowed us to observe how soil mixing and net input varied with climate; which in turned allowed us to better explain C, N and Mn storage trends with MAT. We determined that the diffusive soil mixing rate is increased significantly at sites which receive

large annual precipitation (W and PR) compared to sites which receive only moderate annual precipitation (PA, VA, TN and AL). Due to the simplistic nature of the model, the true input rates of C and N were underestimated. The model –derived input rates for C and N were considered to be “net” input rates; including element loss processes like SOM decomposition as well as true C and N input. The net input rates of C and N decreased with increasing MAT, indicating that the C and N loss rate increases faster than the C and N input rate. The temperature range where the loss rate overtakes the input rate is 11 to 14 °C. This is the area at which our net added C, N and Mn masses begin to decrease; between VA and TN. The Drivas et al. (2011) model provides a simple and adequate explanation for excess Mn storage and transport in soils. It also provides key insight into a first explanation of C and N storage dynamics in varying climates.

Appendix: Full concentration profiles, textural data and soil horizons

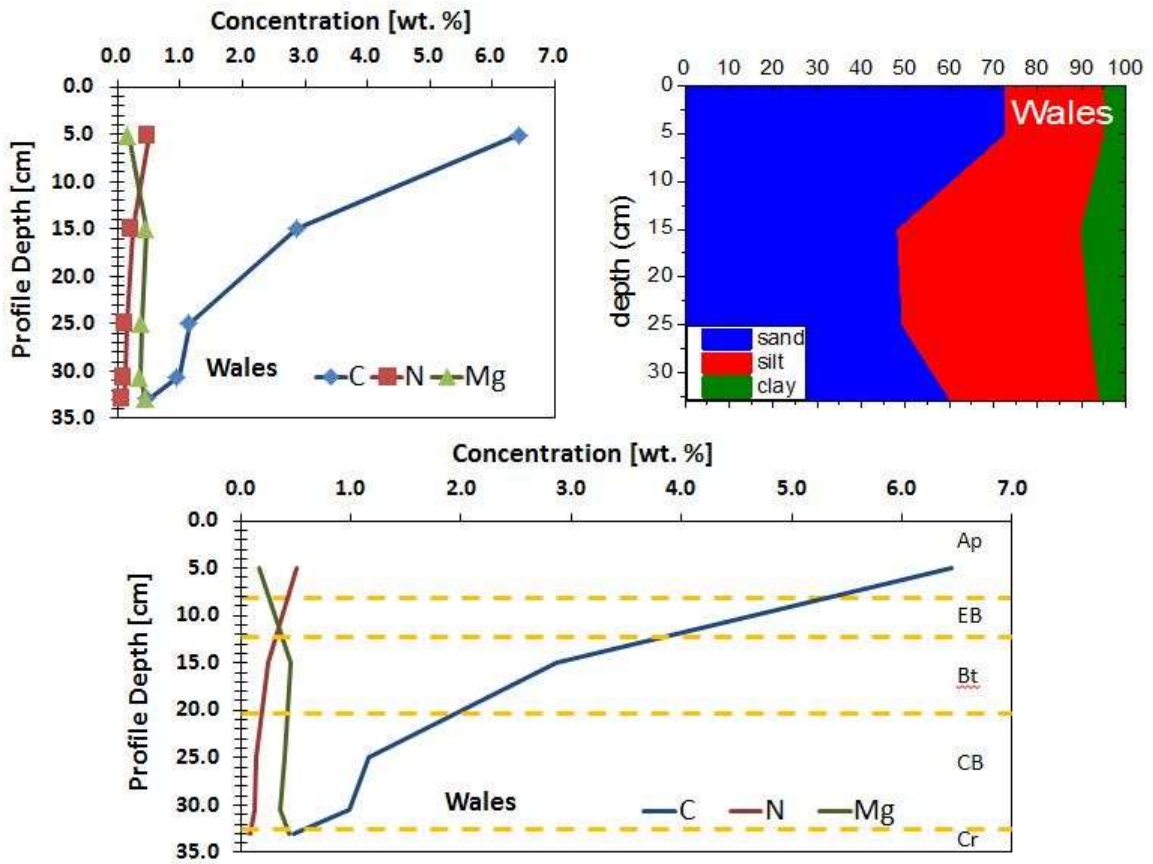


Figure 19. Top: comparison of C, N and Mn concentrations and the soil texture with depth for Wales. Bottom: C, N and Mn concentrations with depth overlain by the taxonomic horizons for Wales.

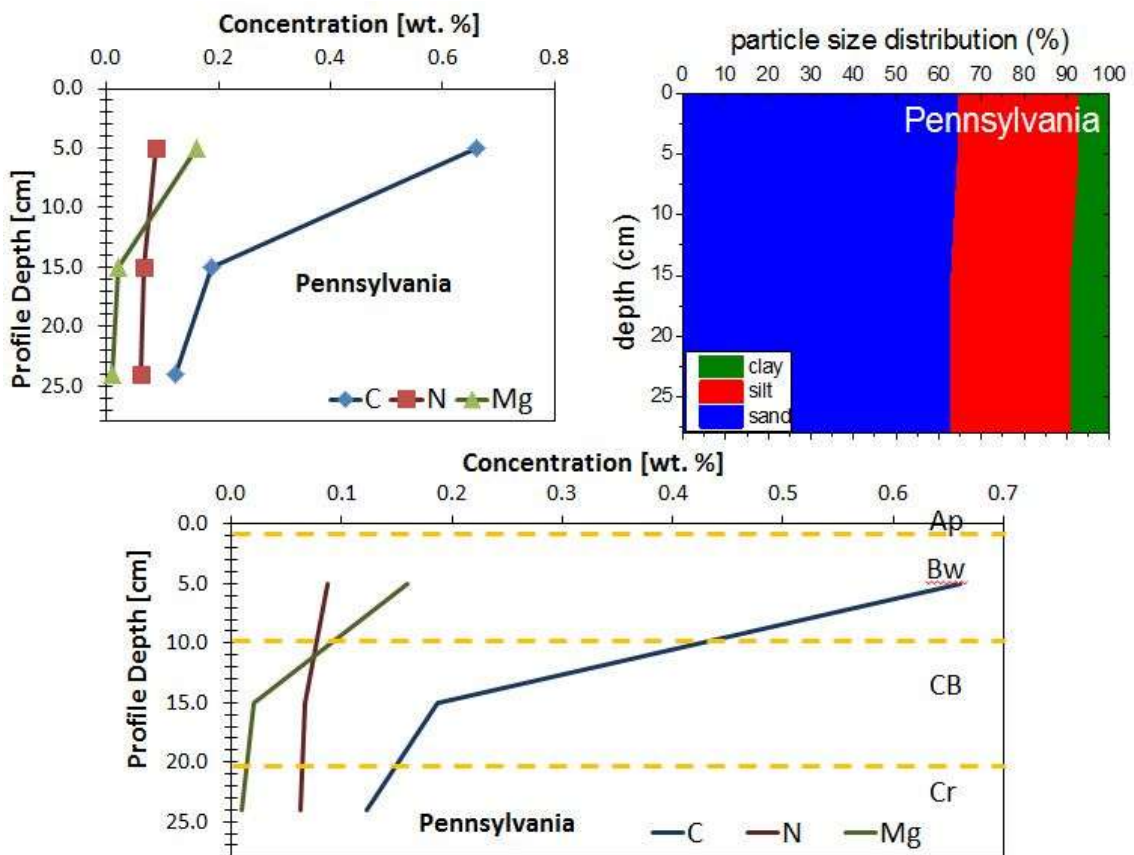


Figure 20. Top: comparison of C, N and Mn concentrations and the soil texture with depth for Pennsylvania. Bottom: C, N and Mn concentrations with depth overlain by the taxonomic horizons for Pennsylvania. *Notice the Bw horizon, indicating a relatively young soil compared to the other samples sites. This could be a possible explanation for the lower C concentrations observed at this site.

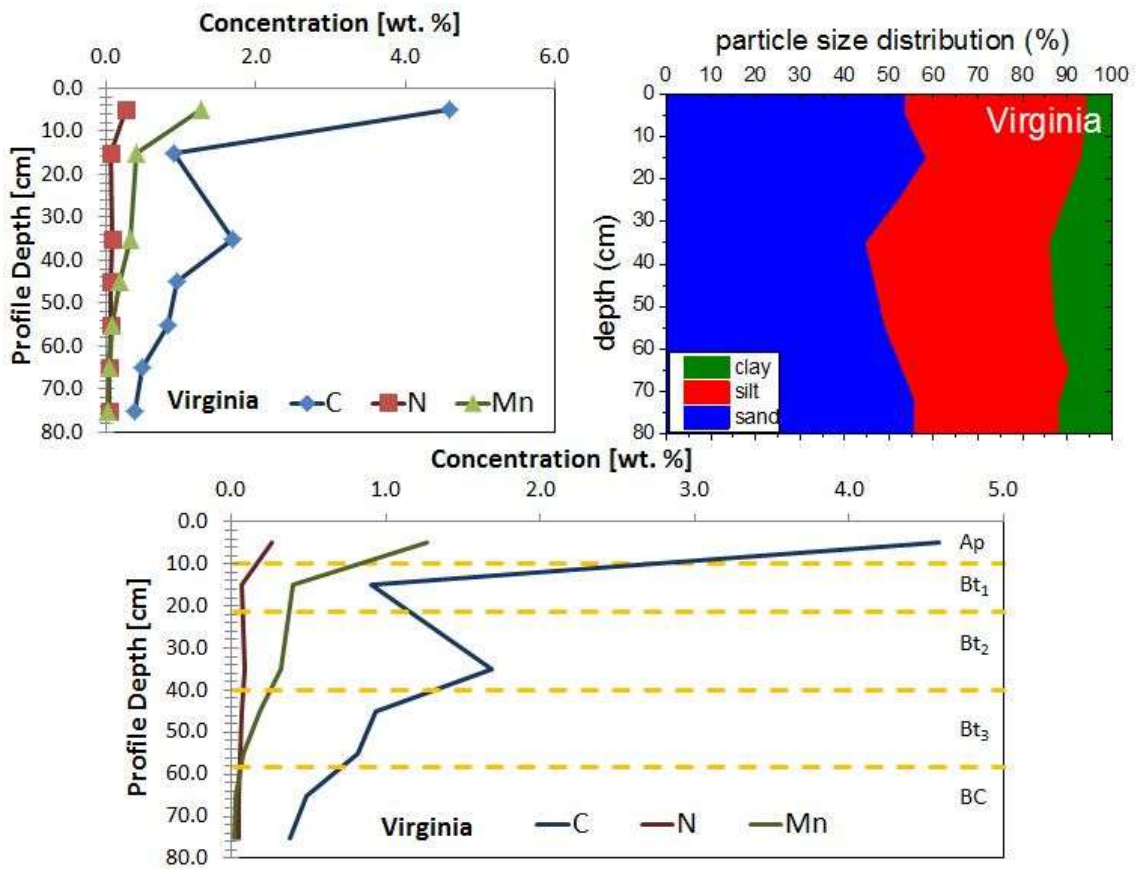


Figure 21. Top: comparison of C, N and Mn concentrations and the soil texture with depth for Virginia. Bottom: C, N and Mn concentrations with depth overlain by the taxonomic horizons for Virginia.

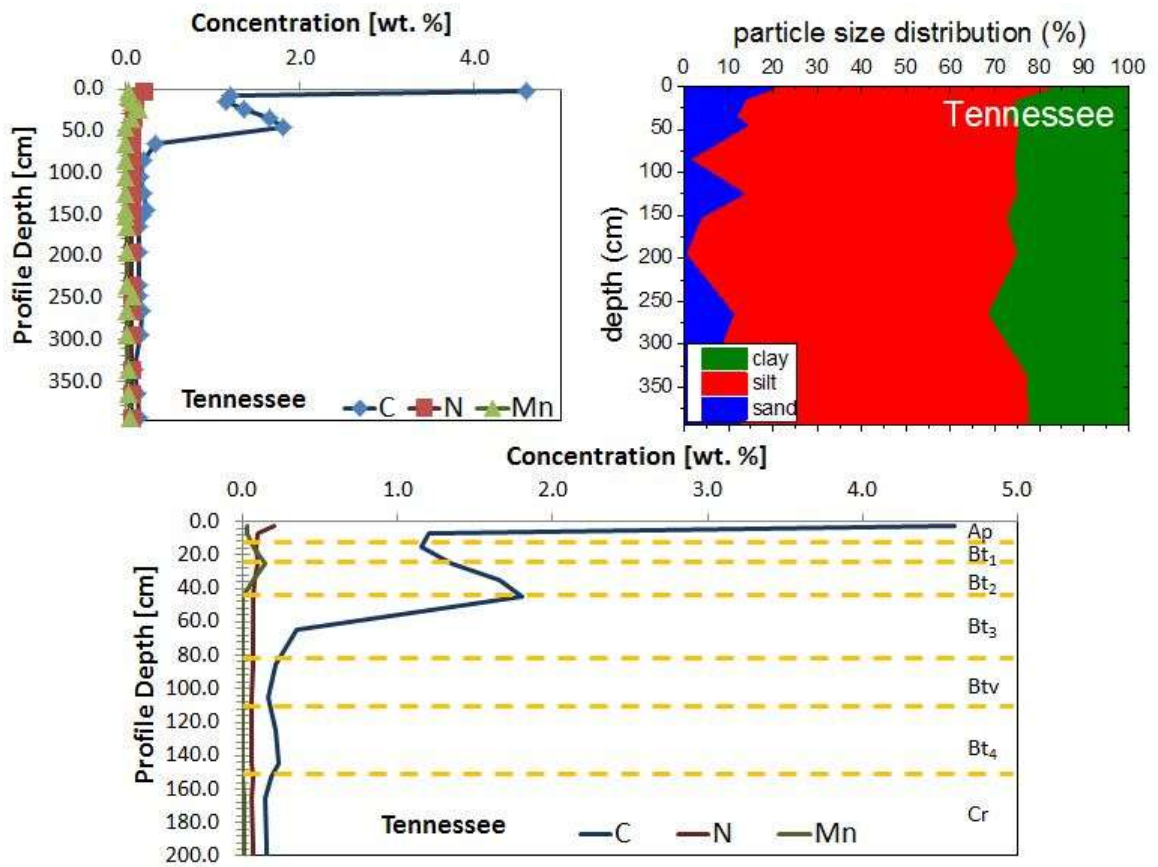


Figure 22. Top: comparison of C, N and Mn concentrations and the soil texture with depth for Tennessee. Bottom: C, N and Mn concentrations with depth overlain by the taxonomic horizons for Tennessee. Notice from the top figure how the concentrations of C, N and Mn are relatively unchanging below 100 cm.

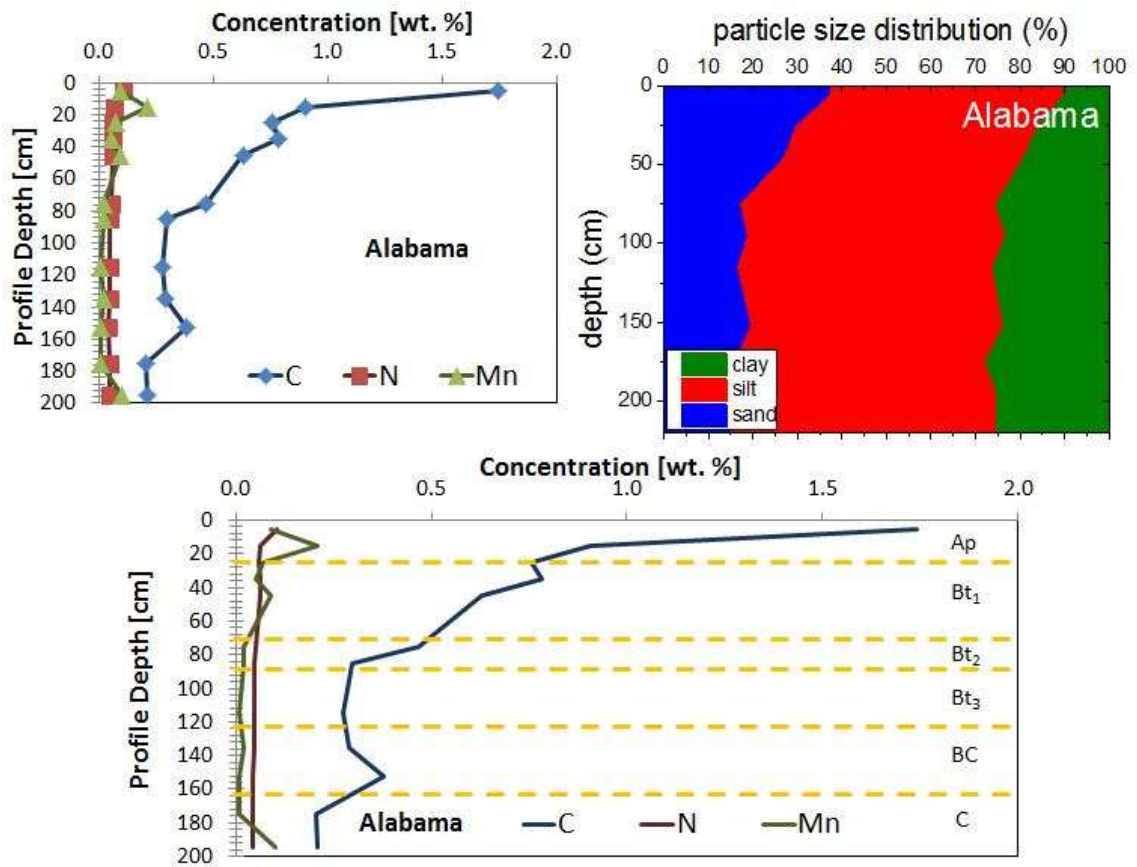


Figure 23. Top: comparison of C, N and Mn concentrations and the soil texture with depth for Alabama. Bottom: C, N and Mn concentrations with depth overlain by the taxonomic horizons for Alabama.

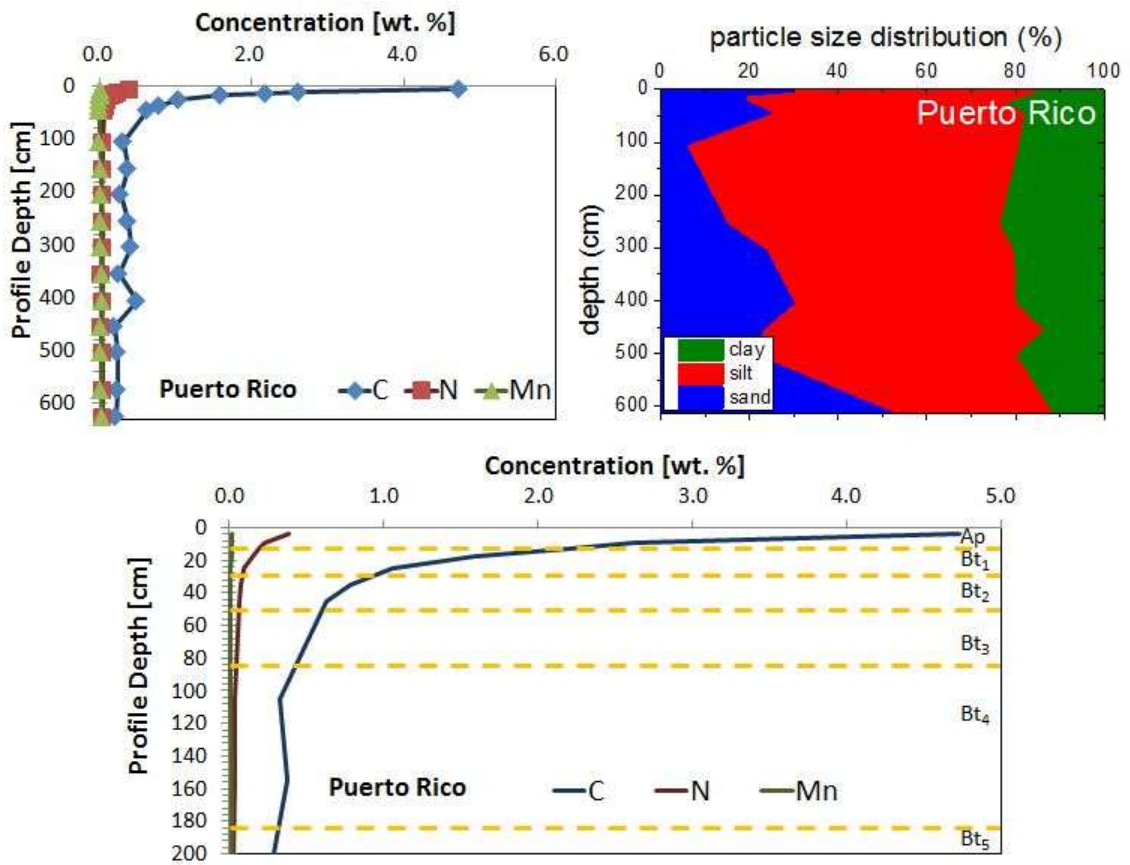


Figure 24. Top: comparison of C, N and Mn concentrations and the soil texture with depth for Puerto Rico. Bottom: C, N and Mn concentrations with depth overlain by the taxonomic horizons for Puerto Rico. Puerto Rico was cropped at 200 cm because the C, N and Mn concentrations were more variable at depth compared to TN.

7. Works Cited

- Anderson, Suzanne Prestrud, William E Dietrich, and George H Brimhall Jr. 2002. "Weathering Profiles , Mass-balance Analysis , and Rates of Solute Loss : Linkages Between Weathering and Erosion in a Small , Steep Catchment." *GSA Bulletin* (9): 1143–1158.
- Baisden, W. T., R. Amundson, D. L. Brenner, a. C. Cook, C. Kendall, and J. W. Harden. 2002. "A Multiisotope C and N Modeling Analysis of Soil Organic Matter Turnover and Transport as a Function of Soil Depth in a California Annual Grassland Soil Chronosequence." *Global Biogeochemical Cycles* 16 (4) (December 20): 82–1–82–26. doi:10.1029/2001GB001823. <http://doi.wiley.com/10.1029/2001GB001823>.
- Booth, Mary S., John M. Stark, and Edward Rastetter. 2005. "Controls on Nitrogen Cycling in Terrestrial Ecosystems: A Synthetic Analysis of Literature Data." *Ecological Monographs* 75 (2): 139–157.
- Braakhekke, Maarten C., Christian Beer, Marcel R. Hoosbeek, Markus Reichstein, Bart Kruijt, Marion Schrumppf, and Pavel Kabat. 2011. "SOMPROF: A Vertically Explicit Soil Organic Matter Model." *Ecological Modeling* 222 (10) (May): 1712–1730. doi:10.1016/j.ecolmodel.2011.02.015. <http://linkinghub.elsevier.com/retrieve/pii/S0304380011000962>.
- Brantley, Susan L., and Marina Lebedeva. 2011. "Learning to Read the Chemistry of Regolith to Understand the Critical Zone." *Annual Review of Earth and Planetary Sciences* 39 (1) (May 30): 387–416. doi:10.1146/annurev-earth-040809-152321. <http://www.annualreviews.org/doi/abs/10.1146/annurev-earth-040809-152321>.
- Brimhall, George H, and William E Dietrich. 1987. "Constitutive Mass Balance Relations Between Chemical Composition, Volume , Density , Porosity , and Strain in Metasomatic Hydrochemkai Systems : Results on Weathering and Pedogenesis." *Geochimica Et Cosmochimica Acta* 51 (4).
- Davidson, Erik, and Ivan Janssens. 2006. "Temperature Sensitivity of Soil Carbon Decomposition and Feedbacks to Climate Change." *Nature*.
- Dere, Ashlee L., Timothy S. White, Rich H. April, Brian Reynolds, Thomas E. Miller, Elizabeth P. Knapp, Larry D. McKay, and Susan L. Brantley. 2013. "Climate Dependence of Feldspar Weathering in Shale Soils Along a Latitudinal Gradient." *In Review*.
- Drivas, Peter, Teresa Bowers, and Roberto Yamartino. 2011. "Soil Mixing Depth after Atmospheric Deposition. 1. Model Development and Validation." *Elsevier: Atmospheric Environment*.
- Elzein, Abbas, and Jerome Balesdent. 1995. "Mechanistic Simulation of Vertical Distribution of Carbon Concentrations and Residence Times in Soils." *Soil Science Society of America Journal*.

- Herndon, Elizabeth M., Lixin Jin, and Susan L Brantley. 2011. "Soils Reveal Widespread Manganese Enrichment from Industrial Inputs." *Environmental Science & Technology* 45 (1) (January 1): 241–7. doi:10.1021/es102001w. <http://www.ncbi.nlm.nih.gov/pubmed/21133425>.
- Herndon, Elizabeth M., and Susan L. Brantley. 2011. "Movement of Manganese Contamination Through the Critical Zone." *Applied Geochemistry* 26 (June): S40–S43. doi:10.1016/j.apgeochem.2011.03.024. <http://linkinghub.elsevier.com/retrieve/pii/S088329271100103X>.
- Jenny, H. 1941. *Factors of Soil Formation: a System of Quantitative Pedology*. McGraw Hill, NY.
- Jin, L., R. Ravella, B. Ketchum, P. Heaney, and S. Brantley. 2010. "Mineral Weathering and Elemental Transport During Hillslope Evolution at the Susquehanna/Shale Hills Critical Zone Observatory." *Geochimica Et Cosmochimica Acta* 74: 3669–3691.
- Jobbagy, Estenban G., and Robert B. Jackson. 2000. "The Vertical Distribution of Soil Organic Carbon and Its Relations Ot Climate and Vegetation." *Ecological Society of America*.
- Kaste, James M., Arjun M. Heimsath, and Benjamin C. Bostick. 2007. "Short-term Soil Mixing Quantified with Fallout Radionuclides." *Geology* 35 (3): 243. doi:10.1130/G23355A.1. <http://geology.gsapubs.org/cgi/doi/10.1130/G23355A.1>.
- Medlin, J.H., N.H. Suhr, and J.B. Bodkin. 1969. "Atomic Absorption Analysis of Silicates Employing LiBO₂ Fusion." *Atmoic Absorption Newsletter* 8: 25–29.
- Parton, W.J., M.B. Coughenour, J.M.O. Scurlock, D.S. Ojima, T.G. Gilmanov, R.J. Scholes, D.S. Schimel, et al. 1996. "Global Grassland Ecosystem Modeling: Development and Test of Ecosystem Models for Grassland System." *SCOPE* 56: 229–266.
- Parton, W.J., M. Hartman, D. Ojima, and D. Schimel. 1998. "DAYCENT and Its Land Surface Submodel." *Global and Planetary Change* 19 (1-4): 35–48.
- SoilSurveyStaff. 1993. *National Soil Survey Handbook, Title 430-VI*. Washington DC: US Government Printing Office.
- U.S E.P.A. 2003. *Health Effects Support Document for Manganese*. Washington DC.
- Yaalon, D.H., and E. Ganor. 1973. "The Influence of Dust on Soils during the Quaternary." *Soil Science Society of America Journal*.

ACADEMIC VITA

Nina Bingham

Address: 145 Goddard Circle Pennsylvania Furnace, PA 16865 email:nlb5110@psu.edu

Education

B.S. Geosciences, 2013

The Pennsylvania State University-University Park, PA

Honors and Awards

- Dean's List, George L. Ellis Scholarship (Earth and Mineral Sciences, 2012), the Marathon Oil Scholarship (Earth and Mineral Sciences, 2009-2013), the Teas Scholarship for Excellence (Earth and Mineral Sciences, 2010) and the James and Nancy Hedberg Scholarship in Geosciences (Department of Geosciences, 2011)

Association Memberships/Activities

- GSA, Geological Society of America
- AAPG, American Association of Petroleum Geologists
- SSSA, Soil Science Society of America

Research Interests

I have a broad interest in soil processes and how to model soil processes using mathematical models. Specifically, I am interested in observing trends in element concentrations of a soil as a proxy for how soil processes are acting on a soil.

Professional Presentations

- Research Poster-2012 SSSA Annual Conference at Cincinnati, Ohio
- Research Poster-2013 Carbon Earth Conference at University Park, Pennsylvania
 - 1st place in undergraduate poster competition